



Optimal Fleet Replacement and Forecasting Under Uncertainty

The CP-140A Arcturus Maritime Surveillance Aircraft

David W. Maybury
Materiel Group Operational Research

DRDC CORA TR 2009–001
March 2009

Defence R&D Canada
Centre for Operational Research and Analysis

Materiel Group Operational Research
Assistant Deputy Minister (Materiel)



National
Defence

Défense
nationale

Canada

Optimal Fleet Replacement and Forecasting Under Uncertainty

The CP-140A Arcturus Maritime Surveillance Aircraft

David W. Maybury
Matériel Group Operational Research

Defence R&D Canada – CORA

Technical Report

DRDC CORA TR 2009–001

March 2009

Principal Author

David W. Maybury

Approved by

R.M.H. Burton
Section Head (Joint and Common OR)

Approved for release by

D.F. Reding
Chief Scientist

© Her Majesty the Queen in Right of Canada as represented by the Minister of National Defence, 2009

© Sa Majesté la Reine (en droit du Canada), telle que représentée par le ministre de la Défense nationale, 2009

Abstract

Using the CP-140A Arcturus maritime surveillance aircraft as a case study, we examine fleet replacement and overhaul decisions by applying the same stochastic techniques used to price financial derivatives. We construct a stochastic fleet replacement/overhaul model with forecasting capabilities for the CP-140A using historical operation and maintenance costs along with historical operational availability trends. Our model uses a class of utility functions based on operational availability for discounting purposes, and the model balances tradeoffs between costs, availability, and uncertainty. We find that the effects of uncertainty in both costs and availability play a non-trivial role in establishing the optimal replacement time. Through the underlying stochastic process driving the fleet costs, we develop forecast envelopes using the parameters of the model. We see this model as having potential for application to other fleets, systems, and subsystems that exhibit stochastic operation and maintenance costs.

Résumé

En étudiant le cas de l'appareil de surveillance maritime CP140A Arcturus, nous examinons les décisions relatives au remplacement et à la révision de la flotte en appliquant les mêmes techniques stochastiques qui servent à fixer les prix des produits dérivés. Nous élaborons un modèle stochastique de remplacement/révision de la flotte assorti de capacités de prévision pour le CP140A à partir des coûts historiques de fonctionnement et d'entretien, ainsi que des tendances historiques de la disponibilité opérationnelle. Notre modèle utilise un ensemble de fonctions de l'utilité basées sur la disponibilité opérationnelle à des fins d'actualisation, et il contrebalance les compromis à faire entre les coûts, la disponibilité et l'incertitude. Nous constatons que les effets de l'incertitude tant du point de vue des coûts que du point de vue de la disponibilité jouent un rôle non négligeable dans l'établissement du délai optimal de remplacement. À partir du processus stochastique sous-jacent qui influence les coûts de la flotte, nous élaborons des enveloppes de prévision fondées sur les paramètres du modèle. Nous estimons que ce modèle pourrait s'appliquer à d'autres flottes, systèmes et sous-systèmes qui exigent des frais stochastiques de fonctionnement et d'entretien.

This page intentionally left blank.

Executive summary

Optimal Fleet Replacement and Forecasting Under Uncertainty

David W. Maybury; DRDC CORA TR 2009–001; Defence R&D Canada – CORA; March 2009.

Repair-replace problems represent a significant challenge for today's Canadian Forces. The practice of retaining fleets for unprecedented long service lives calls for ADM(Mat) to develop a strategy for determining an optimal replacement or major overhaul time. By considering the CP-140A Arcturus maritime surveillance aircraft, we construct a model that signals replacement, modernization, or a "reset-the-clock" overhaul to decision makers. The key assumption of our model is: random events (such as the unexpected discovery of corrosion) occur independently of fleet age, but fleet resiliency diminishes with time, leading to proportionally evolving operation and maintenance (O&M) costs in a random background.

An important feature of the model centers on a fleet wide utility discount as a function of operational availability (Ao) in which we penalize the fleet for unexpectedly low Ao, thereby reflecting the DGAEPM's performance satisfaction. Using the utility function depicted in figure 1, which is risk neutral with respect to increasing Ao on the range of 0% to 100%, figure 2 shows the historical CP-140A O&M cost per utility data superimposed on alternative sample paths generated by the model.

From the data, the model extracts a critical region for the fleet which serves to signal the initiation of a replacement/overhaul decision once the fleet's sample path crosses the lower boundary. Using the critical region of the model for the CP-140A fleet, we learn from figure 3 that the model has already signalled a replacement/overhaul decision for the CP-140A fleet. We also notice that the fleet's O&M cost per utility has received a favourable bump as the sample path has moved toward the lower boundary of the critical region. Since the model values the capacity to delay a decision by properly accounting for the probability of favourable fluctuations, the optimal decision time predicted by our stochastic model is longer relative to deterministic methods. Under the assumption of a passive utility discount, our model predicts:

- The CP-140A entered the critical region for replacement/overhaul decision at year 11 (calendar year 2006), and that the CP-140A sample path has an expectation time to reach the critical region of 11 years (calendar year 2006) after procurement. The 60% confidence interval around the expectation is 6 to 21 years (2001 – 2017). Note that the sample path has not left the critical region in figure 3.
- The passive utility function represents an unbiased expectation of Ao, but always

penalizes the fleet for Ao below 100%. Thus, the result represents a lower bound on all possible passive utility functions.

- Under the assumption that the passive utility function captures the CP-140A fleet's performance expectation, the model calls for the initiation of a replacement/overhaul decision process.

The model allows for other utility function choices. In the paper we present a simple method for constructing a generalized utility functions based on expected fleet Ao performance.

Operational tempo, unforeseen engineering and maintenance problems, and budgeting processes all factor into the evolution of O&M costs of vehicle fleets. Separating specific variables that directly relate to age from other effects presents a daunting task. By treating the problem stochastically under the assumption that fleet resiliency diminishes with time, we can not only predict a probability envelope for the growing costs, but we can also determine the critical time to consider fleet replacement. Most importantly, our approach implicitly attaches a value to the capacity to delay in making the replacement decision – as more information becomes available to the decision makers, better choices can be made. Deterministic methods that focus only on marginal costs ignore this important feature. The model we construct balances economic considerations, uncertainty, and fleet utility in establishing a replacement time. We see the application of stochastic models – similar to the type discussed in this study – to a wide variety of military fleets as fertile ground for future operations research.

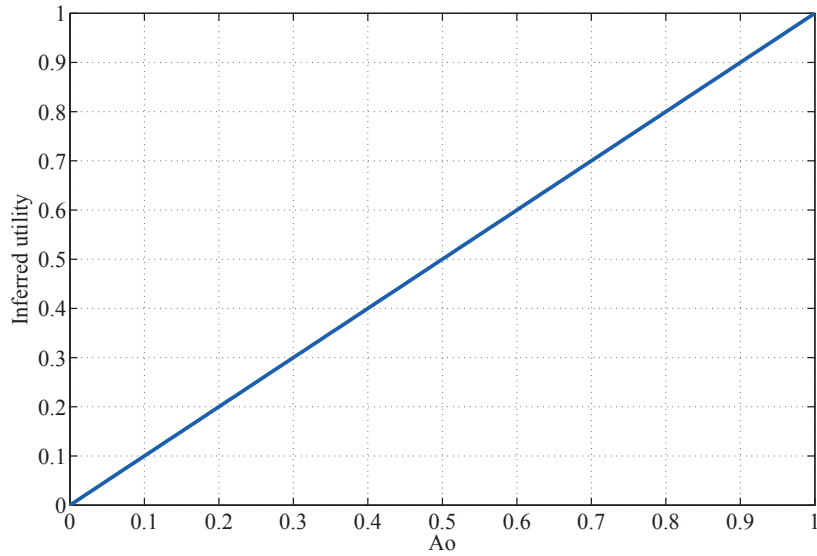


Figure 1: The passive utility function (risk neutral with respect to A_o) used for discounting O&M costs.

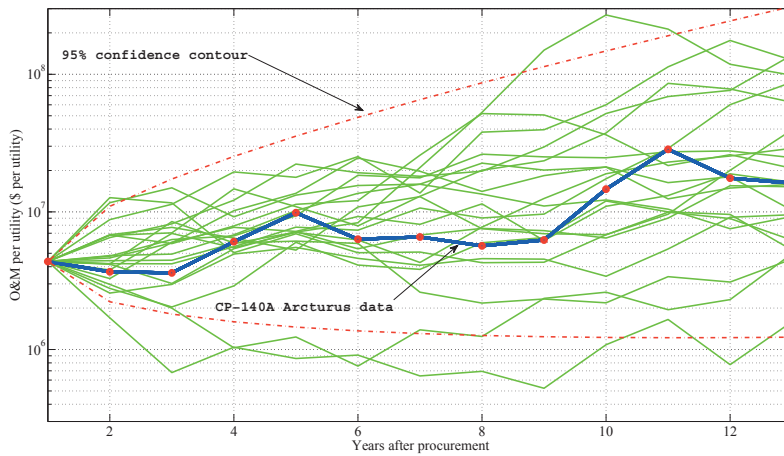


Figure 2: CP-140A Arcturus data superimposed on other possible sample paths generated by the model. The red contour denotes the boundary that contains 95% of all possible sample paths.

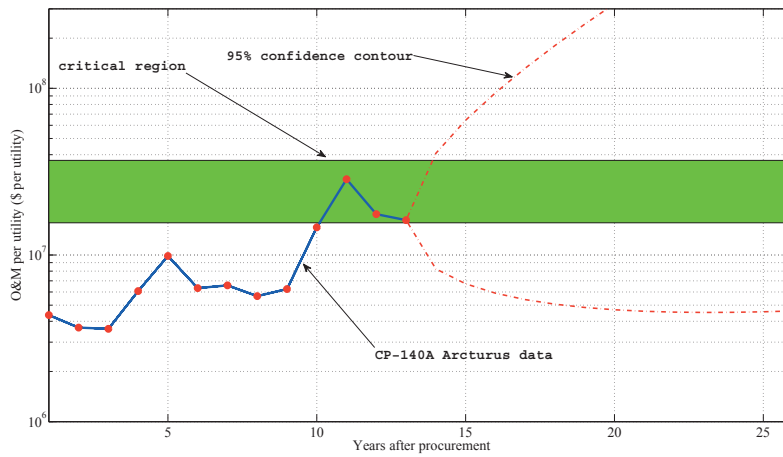


Figure 3: CP-140 Arcturus data with the critical region extracted from the data. Notice that at year 11 the sample path drifted into the critical region only to wander a lower level in the subsequent time steps.

Sommaire

Optimal Fleet Replacement and Forecasting Under Uncertainty

David W. Maybury ; DRDC CORA TR 2009–001 ; R & D pour la défense Canada – CARO ; mars 2009.

Les difficultés de réparation-remplacement posent des défis de taille aux Forces canadiennes d'aujourd'hui. Maintenant que l'on a pris l'habitude de conserver des flottes de navires durant des périodes de service sans précédent, le SMA(Mat) est dans l'obligation d'élaborer une stratégie afin de déterminer le moment optimal du remplacement ou d'une révision générale de son équipement. À partir de l'aéronef de surveillance maritime CP140A Arcturus, nous construisons un modèle qui signale aux décideurs que le moment est venu de procéder au remplacement, à la modernisation, ou à une remise à neuf de l'appareil. Notre modèle repose sur l'hypothèse fondamentale suivante : des événements aléatoires (par exemple la découverte inattendue de corrosion) surviennent peu importe l'âge de l'appareil, mais la résilience de la flotte s'affaiblit au fil du temps, ce qui entraîne des dépenses de fonctionnement et d'entretien (F&E) qui augmentent proportionnellement dans un contexte aléatoire.

Une caractéristique importante du modèle est centrée sur un écart d'actualisation de l'utilité de la flotte au complet, en tant que fonction de la disponibilité opérationnelle (Do) : nous pénalisons la flotte pour une Do plus faible que prévue, de manière à refléter la satisfaction de la DGGPEA à l'égard du rendement. À partir de la fonction de l'utilité illustrée à la figure 4, qui est neutre par rapport au risque d'augmenter la Do de l'ordre de 0% à 100%, la figure 5 montre les coûts historiques de F&E de l'appareil CP140A en superposant les données concernant l'utilité à différentes trajectoires de l'échantillon que génère le modèle.

À partir des données, le modèle délimite une zone critique pour la flotte qui signale la nécessité de prendre une décision de remplacement/révision une fois que la trajectoire de l'échantillon de la flotte traverse la limite inférieure. En utilisant la zone critique du modèle pour la flotte des CP140A, nous constatons à la figure 6 que le modèle a déjà signalé une décision de remplacement/révision pour la flotte des CP140A. Nous remarquons également que le coût du F&E de la flotte par utilité a fait un bond favorable lorsque la trajectoire de l'échantillon s'est approchée de la limite inférieure de la zone critique. Étant donné que le modèle accorde une valeur à la capacité de retarder une décision en tenant dûment compte de la probabilité de fluctuations favorables, notre modèle stochastique prédit une plus longue période optimale de décision que les méthodes déterministes. En prenant l'hypothèse d'une actualisation de l'utilité passive, voici ce que prédit notre modèle :

- Le CP140A est entré dans la zone critique d'une décision de remplacement/révision à l'an 11 (année civile 2006), et selon le délai prévu, la trajectoire de l'échantillon du

CP140A atteindra la zone critique 11 ans après l'acquisition (année civile 2006). L'intervalle de confiance de 60 % à l'égard de l'attente est de 6 à 21 ans (2001 – 2017). À noter que la trajectoire de l'échantillon ne quitte pas la zone critique dans la figure 6.

- La fonction de l'utilité passive représente une attente sans préjugé de Do, mais pénalise toujours la flotte lorsque la Do est inférieure à 100 %. Par conséquent, le résultat représente un seuil inférieur pour toutes les fonctions possibles de l'utilité passive.
- Si l'on suppose que la fonction de l'utilité passive intègre le rendement attendu de la flotte des CP140A, le modèle exige le lancement d'un processus de décision en ce qui concerne le remplacement/la révision.

Le modèle permet d'autres fonctions de l'utilité possibles. Dans la communication, nous présentons une méthode simple d'élaboration de fonctions généralisées de l'utilité selon la Do attendue de la flotte.

La cadence opérationnelle, des difficultés imprévues d'ingénierie et de maintenance, ainsi que les processus budgétaires influencent l'évolution des coûts de F&E des parcs de véhicules. Distinguer les variables qui sont directement liées à l'âge d'autres effets représente une tâche insurmontable. Si nous abordons le problème d'un point de vue stochastique en posant l'hypothèse que la résilience de la flotte diminue avec le temps, nous pouvons non seulement prévoir une enveloppe de probabilité pour la croissance des coûts, mais aussi déterminer à quel moment critique il faut envisager le remplacement de la flotte. Facteur encore plus important, notre méthode accorde implicitement une valeur à la capacité de retarder la décision de remplacement : plus les décideurs ont accès à des renseignements exacts, plus ils sont aptes à faire un choix éclairé. Les méthodes déterministes qui sont axées exclusivement sur le coût différentiel font fi de cette caractéristique importante. Le modèle que nous élaborons contrebalance les considérations économiques, l'incertitude et l'utilité de la flotte en établissant un délai de remplacement. À notre avis, il serait utile que d'éventuels travaux de recherche opérationnelle appliquent des modèles stochastiques - semblables à ceux examinés dans le cadre de cette étude - à toute une gamme de flottes militaires.

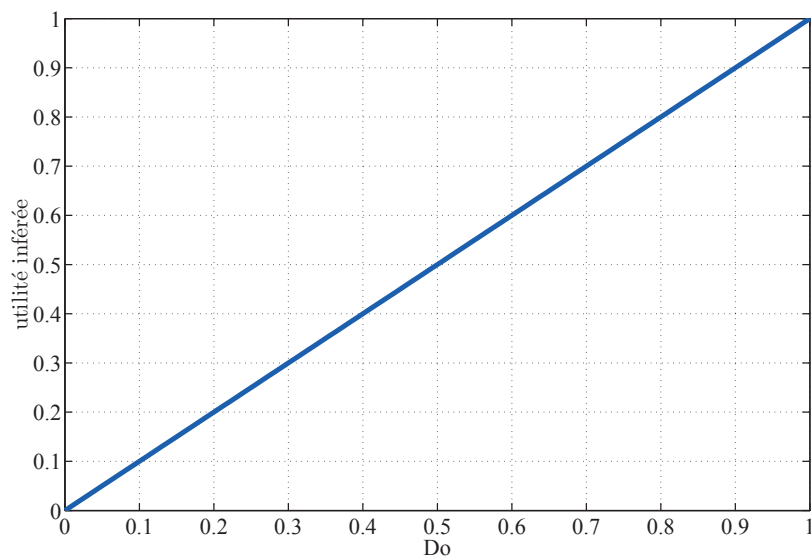


Figure 4: La fonction de l'utilité passive (neutre par rapport au risque pour la Do) sert à actualiser les dépenses de F&E.

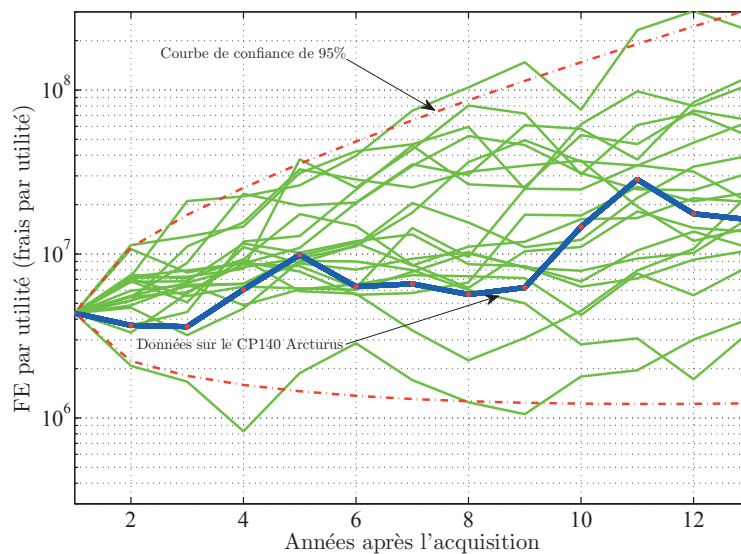


Figure 5: Les données relatives au CP140A Arcturus sont superposées à d'autres trajectoires possibles de l'échantillon généré par le modèle. La courbe rouge marque la frontière qui délimite 95% de toutes les trajectoires possibles de l'échantillon.

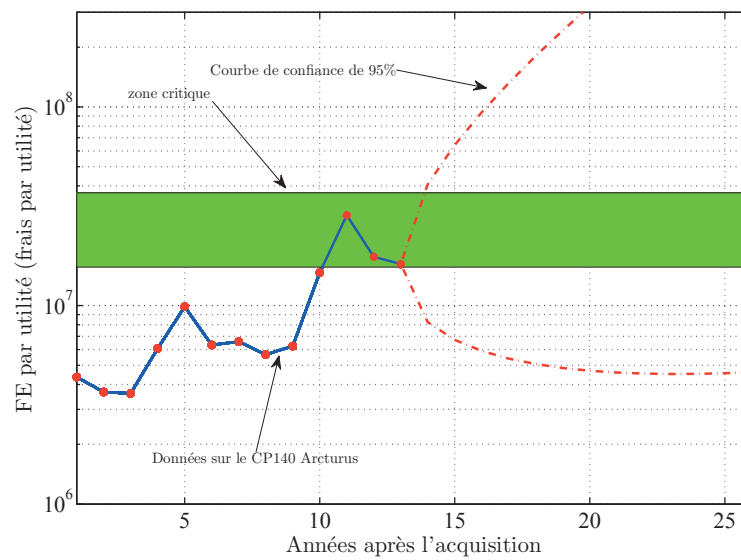


Figure 6: Données sur le CP140A Arcturus et la zone critique obtenue. À noter qu'à la 11e année d'utilisation, la trajectoire de l'échantillon s'est aventurée dans la zone critique mais qu'elle est redescendue par la suite.

Table of contents

| | |
|---|------|
| Abstract | i |
| Résumé | i |
| Executive summary | iii |
| Sommaire | vii |
| Table of contents | xi |
| List of tables | xiii |
| List of figures | xiv |
| Acknowledgements | xvii |
| 1 Introduction | 1 |
| 1.1 Background | 1 |
| 1.2 Scope | 3 |
| 2 The model | 4 |
| 2.1 Deterministic present-value approach | 4 |
| 2.2 The stochastic framework | 6 |
| 2.3 An effectiveness measure | 8 |
| 2.4 The stochastic model | 11 |
| 2.4.1 Expected age | 11 |
| 2.4.2 Expected discount factor | 13 |
| 2.4.3 Expected net present-value | 14 |
| 3 Results: model application to data | 16 |
| 3.1 Data and model assumptions | 16 |
| 3.2 Expected fleet replacement with utility | 18 |
| 3.3 Non-passive utility | 29 |

4 Discussion and conclusions 34

References 37

Annex A: Stochastic differential equations 39

 A.1 Motivation 39

 A.2 Ito’s lemma and stochastic calculus 42

List of Acronyms 46

List of tables

| | | |
|----------|---|----|
| Table 1: | CP-140A Arcturus yearly O&M costs per aircraft and fleet Ao data. Acquisition cost: \$79.6M per aircraft (1993). | 17 |
| Table 2: | Portmanteau test for normality | 21 |
| Table 3: | Additional statistical tests for normality | 22 |

List of figures

| | | |
|------------|---|----|
| Figure 1: | The passive utility function (risk neutral with respect to Ao) used for discounting O&M costs. | v |
| Figure 2: | CP-140A Arcturus data superimposed on other possible sample paths generated by the model. The red contour denotes the boundary that contains 95% of all possible sample paths. | v |
| Figure 3: | CP-140 Arcturus data with the critical region extracted from the data. Notice that at year 11 the sample path drifted into the critical region only to wander a lower level in the subsequent time steps. | vi |
| Figure 4: | La fonction de l'utilité passive (neutre par rapport au risque pour la Do) sert à actualiser les dépenses de F&E. | ix |
| Figure 5: | Les données relatives au CP140A Arcturus sont superposées à d'autres trajectoires possibles de l'échantillon généré par le modèle. La courbe rouge marque la frontière qui délimite 95% de toutes les trajectoires possibles de l'échantillon. | ix |
| Figure 6: | Données sur le CP140A Arcturus et la zone critique obtenue. À noter qu'à la 11e année d'utilisation, la trajectoire de l'échantillon s'est aventurée dans la zone critique mais qu'elle est redescendue par la suite. | x |
| Figure 7: | Inferred expected Ao probability distribution. The range of the plateau is obtained from hypothetical expert opinion (taken here to be 60% – 75%) and linear interpolants are used to match the endpoints of the Ao. The area under the trapezoid profile is constrained to unity. | 9 |
| Figure 8: | Inferred Ao utility function obtained from the cumulant of figure 7. Notice the “S”-shaped curve penalizes the fleet for lower than expected Ao and plateaus for higher than expected Ao. The curve satisfies the requirements of a consistent utility function and is risk prone at lower than expected Ao (willing to forgo guaranteed low Ao for a chance to increase the fleet's performance) and risk averse at higher than expected Ao. | 10 |
| Figure 9: | A passive utility function derived from an uniform expectation. | 19 |
| Figure 10: | The sample autocorrelation function for differences Δx_i . Note that the data lies within the 95% confidence boundaries denoted by the dashed lines. No correlations exists for lags larger than 0. | 22 |

Figure 11: CP-140A Arcturus data superimposed on other possible sample paths generated by the model. The red contour denotes the boundary that contains 95% of all possible sample paths. 23

Figure 12: CP-140 Arcturus data with the critical region extracted from the data. Notice that at year 11 the sample path drifted into the critical region only to wander lower in the subsequent time steps. 24

Figure 13: The probability distribution for the replacement time. The red bar denotes the expected replacement time, while the green bars show the 60% confidence region. Again, we have used the passive utility function. 27

Figure 14: The probability that the CP-140A path, with the passive utility discount, will diffuse through the lower boundary, $L = \$15.6$ million per utility, before the upper boundary, $U = \$36.9$ million per utility, as a function of position inside the critical region. 28

Figure 15: The probability that the CP-140A path will diffuse through the upper boundary $U = \$36.9$ million per utility, before the lower boundary, $L = \$15.6$ million per utility, as a function of position inside the critical region. 29

Figure 16: The probability as a function of time, t , that the CP-140A reaches the critical region starting from the initial procurement data using the passive utility discount. 30

Figure 17: CP-140A Arcturus data superimposed on other possible sample paths generated by the model with the utility function given in figure 8. The red contour denotes the boundary that contains 95% of all possible sample paths. 31

Figure 18: CP-140 Arcturus data with the critical region extracted from the data. Notice that at year 11 the sample path drifted through the critical region only to wander lower in the subsequent time steps. 31

Figure 19: The probability as a function of time, t , that the CP-140A reaches the critical region starting from the initial procurement data using the utility function given in figure 8. 32

Figure 20: The probability that the CP-140A path will diffuse through the lower boundary, $L = \$23.6$ million per utility, before the upper boundary, $U = \$61.0$ million per utility as a function of position inside the critical region, using the utility function in figure 8. 32

Figure 21: The probability that the CP-140A path will diffuse through the upper boundary $U = \$61.0$ million per utility, before the lower boundary, $L = \$23.6$ million per utility, as a function of position inside the critical region, using the utility function in figure 8. 33

Figure 22: The probability distribution for the replacement time with the utility function given in figure 8. The red bar denotes the expected replacement time, while the green bars show the 60% confidence region . 33

Figure A.1: Stochastic behaviour depicted using an Euler-Cauchy approximation. Each time increment contains two pieces: a deterministic drift part and a stochastic fluctuation. 45

Acknowledgements

I am deeply grateful to Dr. G.H. van Bavel, DMGOR 5, for sharing with me his insight regarding suitable Ao measures and for his patient answers to my numerous questions. I am particularly indebted to Colonel R. Foster, COS DGAEPM, and Major P. Appell DAEBM 2-4 for discussions on utility measures. I would also like to thank Professor Cindy Williams of the Massachusetts Institute of Technology, and Mr. Raman Pall, DMGOR 4, for helpful conversations. Finally, I would like to thank Dr. P.E. Desmier, DMGOR, for his encouragement and support over the course of this project.

This page intentionally left blank.

1 Introduction

We have to figure out when it stops making sense to fix some of these old airplanes and it would just be cheaper to buy a new one. — General Michael Ryan, then USAF Chief of Staff (2000)

1.1 Background

Today's Canadian Forces operate increasingly aging military platforms, often retaining fleets for unprecedented long service lives [1]. The unfamiliar territory of operating platforms well beyond expected service lifetimes presents the Department of National Defence with a central problem: to replace a fleet of aging vehicles or to continue an ongoing maintenance regime. As vehicles age, we expect that the overall operating and maintenance costs (O&M) will eventually reach a level prohibitive to continued operation, thereby suggesting vehicle replacement as the best alternative. Aircraft platform replacement decisions arising primarily from aging effects presents a relatively new problem for global militaries. The history of aviation remains a relatively young field, and most replacement decisions in the past have occurred largely through new capability requirements, thus limiting aging effect data. Only recently have selected platforms yielded sufficient data to allow for comprehensive studies.

The United States Airforce (USAF) faces substantial challenges in operating airframes with exceptionally long service lives and, having recognized age as a factor in O&M costs as early as the 1960s [2], the USAF started comprehensive fleet lifetime O&M studies in the 1990s. While limited data in early studies contributed to a confused literature [2]–[4], large data sets and the application of more sophisticated analytical methods available to the USAF in recent years has enabled investigators to draw the cautious conclusion that age effects impact O&M costs. In particular, a 1998 RAND study [5] demonstrated that heavy-maintenance workloads have increased with the chronological age of the KC-135 tanker aircraft, and an earlier RAND study [6] estimated that, for every year increment in the age of a USAF mission design series, O&M costs increase on average by 1.7%. Further studies on age effects using commercial airline data [5], [7], data from US Naval [8]–[11] and US Airforce [6], [12]–[14] aircraft in the areas of workloads, material consumption, repairs per flight hour, mean time between failures, and program depot maintenance all show positive growth with age. Investigators warn [13] that changing accounting practices, budget sluggishness, and relatively fixed maintenance-personnel requirements plague USAF and USN studies, creating a difficult environment in which to extract age effects from other pressures. Raymond Pyles's 2003 RAND corporation investigation for the USAF [13] on the impact of aging airframes on maintenance represents the most comprehensive study to-date. Using regression methods that address several issues simultaneously, Pyles discovered a positive relationship between maintenance requirements – in nearly all activities – with airframe age. Not only did Pyles find that different maintenance tasks realize different age effects for the same airframe, but he also found that age effects correlate with

aircraft complexity and fly-a-way costs.

In light of growing evidence that suggests age impacts maintenance and hence O&M costs, ADM(Mat) requires a strategy to determine the optimal replacement time for a fleet of vehicles after which it becomes increasingly disadvantageous both economically and operationally to maintain the fleet. As a case study for constructing and implementing a strategy for fleet replacement, we consider the CP-140A Arcturus maritime surveillance aircraft. Acquired from the Lockheed Aircraft Corporation by DND in 1993, the CP-140A is the sister aircraft of the CP-140 Aurora, with both airframes based on the P-3 Orion. The Arcturus fleet consists of three vehicles based with 14 Wing at CFB Greenwood and, unlike the Aurora, the Arcturus does not possess anti-submarine warfare capability. Today, the Arcturus finds a primary role in pilot training, drug trafficking interdiction, search-and-rescue, and sovereignty patrols. With a fly-a-way cost of nearly \$80 million dollars (1993), DND expected that the Arcturus would remain in service for 13 years.

Since acquisition, the Arcturus fleet has seen annual O&M costs per vehicle increase from \$2.7 million to \$5.2 million in budget years dollars [15], representing an increase of more than 190%. Discerning pure age effects from the upward spiralling annual O&M costs presents a highly non-trivial problem. Instead of attempting to isolate each age effect from usual inflationary pressures, operational tempo, budget processes, training programs, and random events (such as the discovery of unanticipated maintenance problems), we follow the work of Greenfield et al.[16], [17] by assuming that random events occur independently of airframe age, but that the aircraft's resiliency diminishes with time. Our position maintains that random events trigger O&M costs that evolve proportionally – the aircraft becomes more susceptible to damage as it ages. Our work also extends ideas developed in [15], which uses a deterministic infinite horizon generational replacement model to determine the average fleet age which minimizes total ownership costs. By assuming a more global view of the problem and by focusing on economic considerations that include trade-offs among costs, availability, and the effects of uncertainty, we create a stochastic optimal replacement model. In addition to addressing fleet replacement issues, the model we develop also contains forecasting capabilities, yielding insight into future replacement decisions. Most importantly – and we cannot overstress this point – the model we construct implicitly attaches a value to the capacity to delay a decision. Models based solely on deterministic net present-value arguments implicitly assume that the investment choice is either reversible, in that the investor can cancel the investment if circumstances become unfavourable, or if irreversible, the investment choice occurs as a “now or never proposition”. Few investments occur under these conditions, and the decision to procure a new military platform certainly does not fit the assumptions underlying the deterministic net present-value approach.

1.2 Scope

In this report, we model the O&M costs, appropriately discounting by aircraft operational availability (Ao), using methodologies similar to options pricing in financial derivative markets. In particular, we model growth through a geometric random walk (geometric Brownian motion) and apply the techniques of Ito calculus and dynamic programming. The model we construct represents a prototype for a fleet replacement strategy using data from the CP-140A Arcturus as a case study. In principle, the methods we use to build the model can be applied to broader fleets and to individual systems or sub-systems that exhibit stochastic O&M costs. The DMGOR response to the request by ADM(Mat) for an effective replacement and forecasting model is to:

- demonstrate stochastic modelling techniques with the CP-140A costing and Ao data;
- develop a forecasting method used in conjunction with the fleet replacement strategy; and
- study appropriate Ao discount measures that accurately reflect the client's utility of the vehicle.

We develop our model based on 13 years (1995-2007) of costing and Ao data for the CP-140A Arcturus. We obtained the data from the Cost Factors Manual (CFM) and the PERFORMA database via [15], an earlier study that examines a similar problem.

We organize the paper in four parts. Following the introduction, we present the model in section 2 based on the ideas developed in the Annex on stochastic differential equations. Readers who wish to focus on key results can skip the Annex and related material in section 2. Section 3 applies the model to the CP-140A Arcturus data and provides the reader with two different utility analyses. We also explore the application of mean first passage time methods in section 3, displaying key results in the figures. Finally, in section 4 we present a discussion concerning future research.

2 The model

Empirical evidence suggests a positive relationship between the age of military platforms and their O&M costs [2]–[14]. From a modelling point of view, the most important feature emerging from RAND studies suggests that “many of the problems associated with aging material have emerged with little or no warning”[13]. Thus, the RAND studies lead us to consider stochastic uncertainty in addition to constant growth in O&M costs. Based on the ideas from the literature on forest harvesting and renewable resource management, Greenfield et al. suggest an infinite horizon generational replacement model in the presence of stochastic noise.

Greenfield et al. view the problem of fleet replacement similarly to the problem of deciding to harvest a forest for commercial purposes [19]. As each timber stand grows, it gains in value and, at some point in the future, the forester will make the decision to harvest the stand followed by replanting. Thus, over an infinite time horizon, we see that the forester faces an infinite succession of harvest-replanting cycles. The forester must determine the optimal time interval for harvesting. If all else remains equal over each interval, the first optimal harvest period will be identical to all other periods. The military faces a similar problem in that, as a military platform ages, its O&M costs increase, eventually leading to a necessary replacement. We can imagine that the military enters a series of repair-replace cycles and, like the forester, the military must determine the optimal interval for replacement.

In order to develop intuition with the model of Greenfield et al. [16], we will develop the model in stages through the following subsections. We first present the deterministic infinite horizon generational replacement model (see [20] for contextual examples of replacement models of this type) followed by a description of the necessary ingredients required to promote the model to a stochastic version. In addition, the following subsections will elucidate our model extension by discussing a platform effectiveness measure in detail. Finally, we will assemble all components in subsection 2.4 to generate the full stochastic model. The reader who does not wish to explore the model construction can skip the remainder of this section.

2.1 Deterministic present-value approach

In a deterministic universe in which we exactly know the fleet O&M costs evolution function, we can construct a model [15]–[17] that determines the exact replacement time. Let us assume that a military platform has an acquisition cost p , in an environment of a continuously compounding interest rate discount r , with an instantaneous (known) O&M cost rate, $m(t)$. The variable t denotes the chronological age of the platform and s denotes the replacement time. We assume that the military looks to minimize total ownership costs, thereby determining an appropriate replacement time. The net present-value life-cycle cost

of a fleet generation reads

$$p + \int_0^s dt m(t) \exp(-rt). \quad (1)$$

We now imagine that the replacement process repeats ad infinitum. Like the forester's problem, if all else remains equal, each generation faces the same O&M cost structure. Thus, we can write the total ownership cost of successively owning a series of fleets,

$$c(s) = \sum_{i=0}^{\infty} \left(p + \int_0^s dt m(t) \exp(-rt) \right) \exp(-rsi). \quad (2)$$

The total ownership cost, eq.(2), represents a converging geometric series yielding,

$$c(s) = \frac{p + \int_0^s dt m(t) \exp(-rt)}{1 - \exp(-rs)}. \quad (3)$$

Differentiating this expression with respect to the replacement time, s , we find that the military minimizes total ownership cost through the optimality condition

$$m(s^*) = rp + r \frac{\left(\int_0^{s^*} dt m(t) \exp(-rt) \right) + p \exp(-rs^*)}{1 - \exp(-rs^*)}. \quad (4)$$

The critical time s^* can be found numerically. As an example, if we know that the instantaneous O&M cost rate has the form $m(t) = b \exp(\alpha t)$, then we find that

$$c(s) = \frac{p + \frac{b(1 - \exp(-(r-\alpha)s)}{r-\alpha}}{1 - \exp(-rs)} \quad (5)$$

and

$$m(s^*) = b \exp(\alpha s^*) = rp + r \frac{\frac{b(1 - \exp(-(r-\alpha)s^*))}{r-\alpha} + p \exp(-rs^*)}{1 - \exp(-rs^*)} \quad (6)$$

Again, we can find s^* numerically.

While the forest harvester's model assumes that DND replaces the fleet with exactly the same vehicle at exactly the same price in constant dollars, we caution the reader that the model does not assume this situation reflects reality. The model simply determines the total ownership cost associated with the *specific* vehicle under consideration. One cannot compare a different platform with the current fleet if we seek to understand the total ownership cost of the fleet in question. The infinite horizon generational replacement model determines the total ownership cost curve associated with the fleet under consideration. In this regard, the model determines the point at which the fleet no longer provides value, given that the fleet can be replaced in light of the cash flow required to sustain it.

The problem with the model outlined thus far stems not from its lack of a replacement option comparison, but from the assumption of an exactly known O&M cost evolution.

While the model recognizes the irreversibility of the replacement decision, it implicitly assumes that the decision to replace occurs as a now or never proposition. According to the solution given in eq.(6), every year the military retains the fleet past $t = s^*$, DND incurs a known marginal cost. Thus, the model demands replacement at exactly time $t = s^*$ – the now or never situation. In reality, not only do we not know the actual O&M cost evolution, we do not even know for certain what level the O&M costs will reach in the following year. Since the costs evolve stochastically, there is a chance that the following year will see a *decrease* in O&M costs from random occurrences. (This situation is not too difficult to imagine – suppose that the worldwide price of an essential commodity in airframe component manufacturing deflates dramatically.) The chance that the O&M costs can actually decrease in the next year – no matter how small – must factor into our decision to replace the fleet. We require a model that places a value on the capacity to wait. The model must tell us that replacement becomes advantageous only when an appropriate combined initial investment cost and waiting value barrier is crossed.

2.2 The stochastic framework

The infinite horizon generational replacement model views the fleet ownership problem as an infinite series of replacements and determines the optimal replacement interval by minimizing the total ownership cost. If all things remain equal throughout the infinite series, the optimal replacement time for the first interval will also be the optimal replacement time for all subsequent replacements. Following the work of Greenfield et al. [16], and using the RAND observation that failures often occur unexpectedly, we assume that O&M costs evolve proportionally with time, driven in part by random events (including component market price fluctuations) that occur independently of airframe age. By also assuming that the aircraft’s resiliency diminishes with age, the random events have a compounding effect with time, leading to a geometric random walk (Brownian) model of O&M costs, described by the stochastic differential equation

$$dm = \alpha m dm + \sigma m dW(t) \quad (7)$$

where α denotes the growth parameter and $dW(t)$ denotes the Weiner process (see Annex). Note that the Weiner process evolves proportionally to the constant parameter σ and the current level of the O&M costs. In this sense, we imagine the O&M costs evolving not unlike a stock or financial derivative. Following A.2, we see that the Weiner process in eq.(7) implies that the path $m(t)$ is nowhere differentiable, and hence the analysis of the previous section, in which we differentiated the total ownership curve to find the optimal replacement time, cannot apply. We must apply a new set of tools that address the stochastic nature of the problem.

Instead of attempting to determine the expected age of fleet replacement directly, we can approach the problem from a dynamic programming point of view. The decision to replace a fleet of vehicles or to hold the fleet for one more time increment constitutes a series of

optimal replacement problems. Using Bellman's principle (see for example [21]), which states that, whatever the initial action in an optimal policy problem, the remaining choices constitute another optimal policy problem starting from the state that results after the initial action, we can construct a recursive set of stochastic differential equations to solve the replacement problem. As an example, let $F(x_i)$ denote the value of a financial instrument at time t_i based on the value of some state variable x_i , which might be the price of a more basic asset such as a stock, a bond, or a bushel of wheat. We now imagine that we have a set of choices available to us, such as to sell or to hold our financial instrument, that we can label through a control variable u_i . If we denote the immediate payoff of the instrument at t_i by $\pi_i(x_i, u_i)$, then the total value of the instrument – including the value of continuation (discounted back to today with interest rate, r) – becomes¹

$$V_i = \pi_i(x_i, u_i) + \frac{1}{1+r} \mathbf{E}(F(x_{i+1})) \quad (8)$$

The second term in eq.(8) explicitly values the option to continue holding the instrument. We seek to make successive decisions, labelled by u_i , that maximize $F(x_i)$:

$$F(x_i) = \max_{u_i} \left[\pi_i(x_i, u_i) + \frac{1}{1+r} \mathbf{E}(F(x_{i+1})) \right] \quad (9)$$

and in the continuum limit, we obtain the recursive structure

$$F(x) = \max_{u_i} \left[\pi_i(x, u_i) + \frac{1}{1+r} \mathbf{E}(F(x')|x, u) \right]. \quad (10)$$

where the last term denotes the conditional expectation. Using the ideas developed thus far, we can extend Bellman's equations by redefining $\pi(x, u, t)$ as a cash flow rate and thus in time increment Δt , we now have

$$F(x, t) = \max_{u_i} \left[\pi(x, u, t) \Delta t + \frac{1}{1+r\Delta t} \mathbf{E}(F(x', t + \Delta t)|x, u) \right]. \quad (11)$$

Multiplying by $1 + r\Delta t$ and letting $\Delta t \rightarrow 0$ we find

$$rF(x, t) = \max_{u_i} \left[\pi(x, u, t) + \frac{1}{dt} \mathbf{E}(dF) \right]. \quad (12)$$

We will use eq.(12) in our replacement analysis. Note that by using Bellman equations, we have attached a value to future expectation. By phrasing our fleet replacement problem through the lens of an optimal policy problem, we see that uncertainty plays a non-trivial role in the final decision.

¹We will use $E(\cdot)$ to denote the expectation operator throughout.

2.3 An effectiveness measure

Before extending the analysis further, we require a measure that captures the effectiveness of the military platform for discounting purposes. In an investment decision, the “effectiveness” of the project usually involves an expected cash flow or the expectation of financial growth. From a military point of view, effectiveness measures less tangible capacities such as mission readiness, operational availability and, in the case of aircraft, the ability to perform a quality flying hour. Previous studies [14] have addressed the issue of availability measures for the purposes of discounting which aim to ensure that the optimal replacement decision involves tradeoffs between costs and performance. In this section, we expand on this concept.

Based on discussions with DGAEPM staff [22], [23], we construct a measure of effectiveness based solely on operational availability (A_o). The Canadian Forces maintain detailed records on A_o on all aircraft in the PERFORMA database². Each time maintainers open a work ticket on a vehicle, the vehicle becomes unavailable and remains so until the ticket closes. The PERFORMA definition of A_o reads

$$A_o = \frac{\text{uptime}}{\text{uptime} + \text{downtime}}. \quad (13)$$

Since the Canadian Forces maintain detailed engineering records that yield reliable A_o data, we feel that an effectiveness measure based on A_o will produce a robust estimate of platform performance. In addition to A_o , we require a subjective utility measure of the A_o itself. Put simply, the military might regard a platform with A_o of 20% as nearly equivalent to an A_o of 1% since the the ability to perform on military operations might be equally compromised in each case. Conversely, the military might view 85% and 90% A_o as roughly equivalent because the increased availability does not substantially impact operations. Extracting this subjective utility, $U(A_o)$, from the military represents a daunting task. Our discussions with DGAEPM staff suggest that if we polled many experts on the functional form of $U(A_o)$, we would find a wide variety of answers with large discrepancies. Furthermore, in reality, if the A_o of a platform drops, the planners augment their objectives to match the lower expected A_o . This feedback further confuses the ability to extract a robust utility. We therefore suggest an alternative method for extracting $U(A_o)$ from military planners.

While experts will disagree on their choices for the functional form of $U(A_o)$ we imagine that they can agree on their expectation of the availability of the platform at the point of initial procurement. In particular, once DND obtains a new fleet, military planners will expect that the average availability of the fleet over any given year will lie in a certain range

²We consider A_o to be a top-level performance indicator. Aircraft utilization as well as personnel experience level, facilities, sparing, change in publications, policy changes, and test equipment all have a strong influence on the resulting A_o . Since many different factors influence A_o (including errors), we treat A_o fluctuations as random events within the stochastic model.

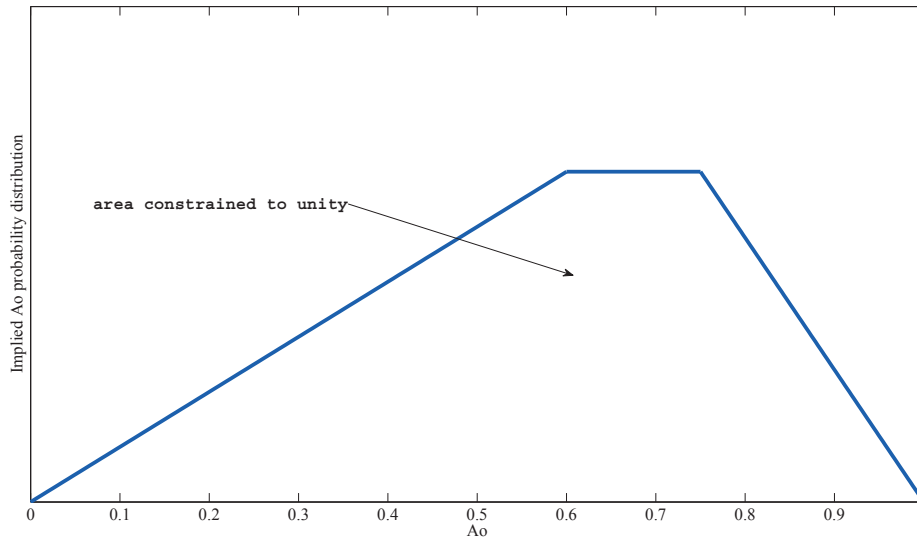


Figure 7: Inferred expected Ao probability distribution. The range of the plateau is obtained from hypothetical expert opinion (taken here to be 60% – 75%) and linear interpolants are used to match the endpoints of the Ao . The area under the trapezoid profile is constrained to unity.

of Ao and plan accordingly. We imagine that experts can reach a consensus regarding this expected Ao range. If we suppose that experts tailor initial planning around an expected Ao , this figure represents a “best guess” estimate of the most probable outcome and thus represents a slice of a probability distribution. Using this consensus, we interpret the expert’s range as part of a probability distribution with a simple trapezoid profile (see figure 7). From this probability distribution, we use the cumulant of the trapezoid distribution as an *inferred* utility function, $U(Ao)$. From figure 8, we see that the utility function possesses the property of monotonicity with the subjectively pleasing feature that unexpectedly low Ao and unexpectedly high Ao approach 0 and 1 respectively. We also note that the trapezoid profile yields a convex utility curve prior to the plateau in figure 7 and a concave curve after the plateau. From a utility theory standpoint, the utility curve implies a high risk tolerance with lower than expected Ao (i.e., willing to forgo guaranteed low Ao for a chance to increase the fleet’s performance), but risk averse once the fleet performs above expectation. In the remainder of this paper we examine not the O&M costs evolution, but the evolution of O&M costs per utility.

While the trapezoid profile in figure 7 extends from 0% to 100%, a given fleet will have a realistic upper Ao bound lower than 100%. Prescribed maintenance activities and warranty inspections will involve aircraft downtime, thereby preventing the fleet from ever attaining 100% Ao . Thus, in reality, the trapezoid profile will have a cutoff below the 100% level.

We caution that in order to use the effectiveness measure for discounting purposes, military planners must arrive at a consensus on the utility function. The consensus will involve *subjective* professional opinions on the location of the trapezoid plateau, the range of the plateau, and the trapezoid cutoff. For case study purposes, we will let the trapezoid profile run from 0% to 100% which will establish lower bounds on the replacement/overhaul decision time for utility functions in a given class.

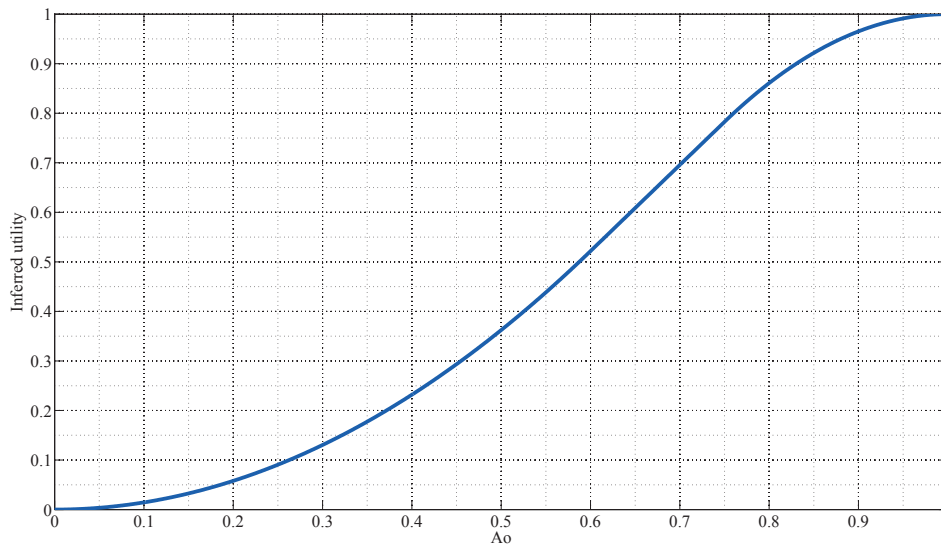


Figure 8: Inferred Ao utility function obtained from the cumulant of figure 7. Notice the “S”-shaped curve penalizes the fleet for lower than expected Ao and plateaus for higher than expected Ao. The curve satisfies the requirements of a consistent utility function and is risk prone at lower than expected Ao (willing to forgo guaranteed low Ao for a chance to increase the fleet’s performance) and risk averse at higher than expected Ao.

2.4 The stochastic model

Having constructed the utility measure as a function of Ao , we can now apply an appropriate discounting procedure to the O&M random process. We assume that O&M per utility ($O\&M/U(Ao)$) follows a geometric random walk described by the process³

$$dm_u = \alpha m_u dt + \sigma m_u dW \quad (14)$$

in which m_u denotes the O&M cost per utility. We see that eq.(14) represents a simple modification of eq.(7) in that $m_u(t) = m(t)/U(Ao)$.

2.4.1 Expected age

We are now in a position to determine the expected age of replacement. First, we imagine a pre-determined cut-off cost per utility (perhaps set independently by policy) m_u^* , above which DND is not willing to pay. Once we find $m_u > m_u^*$, we consider fleet replacement or a reset-the-clock overhaul. Later in this section we will see how we can determine an optimal cutoff based on the parameters of the model. We imagine that the process starts at initial condition b below m_u^* and, using Bellman's recursive equation from the last section, we see that the expected age, $a(m_u^*, m_u)$ evolves as,

$$a(m_u^*, m_u) = dt + (a(m_u^*, m_u) + E(da(m_u^*, m_u))). \quad (15)$$

Note that eq.(15) contains two parts: an additive time increment in the expected age from the current time increment, and a term that represents the expected age at replacement resulting from the time increment. After some manipulation, we can re-express eq.(15) as

$$\frac{E(da(m_u^*, m_u))}{dt} + 1 = 0; \quad (16)$$

Expanding the differential using Ito's Lemma (see Annex) we find

$$E(da(m_u^*, m_u)) = \left(\frac{1}{2} \sigma^2 m_u^2 \frac{d^2 a(m_u^*, m_u)}{dm_u^2} + \alpha m_u \frac{da(m_u^*, m_u)}{dm_u} \right) \quad (17)$$

where we have used $E(dW) = 0$. Thus, we have the differential equation for the expected age of replacement,

$$\frac{1}{2} \sigma^2 m_u^2 \frac{d^2 a(m_u^*, m_u)}{dm_u^2} + \alpha m \frac{da(m_u^*, m_u)}{dm_u} + 1 = 0 \quad (18)$$

³The assumption of geometric random walk behaviour for m_u must be check empirically. In reality, Ao will have its own bounded (0% and 100%) stochastic evolution. The stochastic properties of Ao , and hence $U(Ao)$, can in principle drive the ratio process, m_u , away from a geometric random walk. In full generality, we should not expect m_u to follow a geometric random walk – especially if the stochastic properties of $U(Ao)$ possess strong non-Gaussian fluctuations. This model approximates m_u as a geometric random walk and performs statistical tests with the data to determine if the approximation provides a good description of the process.

We should note that, while we obtained eq.(18) through dynamic programming, we could have obtained the same result from a mean first passage time approach. If we regard the cutoff, m_u^* , as a barrier, the problem amounts to finding the expected time for m_u to diffuse from some initial starting point to the barrier. The stochastic formalism requires the backward Fokker-Planck equation obtained from eq.(14) and, in this case, results in eq.(18) (see Annex for details). Thus, we can approach the replacement problem from either perspective, and we will use either formalism as appropriate. Since $m_u = 0$ is an absorbing point in the geometric random walk, the solution to eq.(18) reads,

$$a(m_u^*, m_u) = A + B \ln(m_u). \quad (19)$$

If we assume the initial condition $m_u(t = 0) = b$ along with the boundary condition that the expected age at m_u^* vanishes, $a(m_u^*, m_u^*) = 0$, we find the expected time for platform replacement,

$$a(m_u^*, b) = \frac{\ln(m_u^*/b)}{\alpha - (1/2)\sigma^2}. \quad (20)$$

Again, we can obtain the same result from calculating the mean first passage time of $a(m_u^*, m)$ from b through the barrier m_u^* .

Eq.(20) connects with the deterministic approach since setting $\sigma = 0$ recovers the deterministic result. In the deterministic case, we find the exact age at which to replace the vehicle as a function of the pre-determined boundary, m_u^* , namely

$$a(m_u^*, b) = \frac{1}{\alpha} \ln(m_u^*/b). \quad (21)$$

The deterministic case determines m_u^* through eq.(6). Thus, we see that uncertainty in the system, characterized by σ , demands that we hold the platform longer than the deterministic result. We see that the stochastic approach implicitly values the capacity to wait by recognizing that there is a chance that next year's O&M cost per utility will decrease. The term σ reflects the size of this chance and thereby increases the waiting time. We also notice that in order for the eq.(20) to make sense, we must have $\alpha - (1/2)\sigma^2 > 0$, otherwise the expectation time to cross the barrier m_u^* becomes infinite (implying that it will never be advantageous to replace the vehicle).

We can go further in the connection between the deterministic and stochastic approaches. If $\sigma = 0$, the stochastic part of the model vanishes, and we are left with the deterministic total ownership cost curve. In the model under consideration, we have exponential growth of OM costs, hence

$$c(s) = \frac{p + \frac{b(1 - \exp(-(r-\alpha)s)}{r-\alpha}}{1 - \exp(-rs)} \quad (22)$$

where the parameters are defined as in section 2.1. Notice that the second term in the numerator behaves as the total net present-value of the generation at time $s = s^*$ and notice

that the denominator acts as the total discount factor at $s = s^*$. In the stochastic case, we can use the Bellman equations of dynamic programming to determine the expected discount factor and the expected total net present-value at replacement respectively.

2.4.2 Expected discount factor

The expected discount factor at replacement proceeds in a similar fashion to the expected age calculation except that we no longer have an additive increment since the discount factor appears multiplicative in the total ownership relation. Thus, we have the following Bellman equation for the expected discount factor

$$\rho(m_u^*, m_u) = \exp(-rdt) [\rho(m_u^*, m_u) + E(d\rho(m_u^*, m_u))]. \quad (23)$$

Rearranging, we find

$$E(d\rho(m_u^*, m_u)) + (1 - \exp(rdt))\rho(m_u^*, m_u) = 0 \quad (24)$$

and, with the use of Ito's Lemma, we have

$$E(d\rho(m_u^*, m_u)) = \left(\frac{1}{2} \sigma^2 m_u^2 \frac{d^2 \rho(m_u^*, m_u)}{dm_u^2} + \alpha m_u \frac{d\rho(m_u^*, m_u)}{dm_u} \right) dt = 0. \quad (25)$$

Altogether, we find that the expected discount factor obeys

$$\frac{1}{2} \sigma^2 m_u^2 \frac{d^2 \rho(m_u^*, m_u)}{dm_u^2} + \alpha m_u \frac{d\rho(m_u^*, m_u)}{dm_u} - r\rho(m_u^*, m_u) = 0. \quad (26)$$

Eq.(26) is an Euler-Cauchy differential equation and therefore has the solution,

$$\rho(m_u^*, m_u) = Am_u^{\beta_1} + Bm_u^{\beta_2}. \quad (27)$$

Substituting our solution into eq.(26) we obtain β_1, β_2 as the roots of the quadratic equation,

$$\frac{1}{2} \sigma^2 (\beta - 1)\beta + \alpha\beta - r = 0, \quad (28)$$

namely,

$$\beta_{1,2} = - \left(\frac{\alpha}{\sigma^2} - \frac{1}{2} \right) \pm \sqrt{\left(\frac{\alpha}{\sigma^2} - \frac{1}{2} \right)^2 + \frac{2r}{\sigma^2}}. \quad (29)$$

The boundary condition

$$\rho(m_u^*, 0) = 0 \quad (30)$$

demands that the coefficient associated with negative root vanishes, and the boundary condition,

$$\rho(m_u^*, m_u^*) = 1 \quad (31)$$

implies that $A = (m_u^*)^{-\beta_1}$. Thus, the full solution for the expected discount factor at replacement, in light of the boundary conditions, reads

$$\rho(m_u) = \left(\frac{m_u}{m_u^*} \right)^{\beta_1}. \quad (32)$$

2.4.3 Expected net present-value

We can approach the expected net present-value of the life-cycle cost similarly. In this case, the recursive Bellman equation contains an additive term as the O&M cost per utility accrues over time,

$$M(m_u^*, m_u) = m_u dt + \exp(-rdt) (M(m_u^*, m_u) + E(dM(m_u^*, m_u))) \quad (33)$$

Applying Ito's Lemma once more, we find the differential equation,

$$\frac{1}{2} \sigma^2 m_u^2 \frac{d^2 M(m_u^*, m_u)}{dm_u^2} + \alpha m_u \frac{dM(m_u^*, m_u)}{dm_u} - rM(m_u^*, m_u) + m_u = 0. \quad (34)$$

In this case we have an inhomogeneous Euler-Cauchy differential equation, and applying the boundary conditions $M(m_u^*, m_u^*) = 0$ (i.e. the life-cycle cost goes to zero as the cycle has ended) and $M(m_u^*, 0) = 0$, and including the starting value, b , at the beginning of the cycle, we find

$$M(m_u^*, b) = \frac{b}{r - \alpha} \left(1 - \left(\frac{b}{m_u^*} \right)^{\beta_1 - 1} \right). \quad (35)$$

If we now put the expected net present life-cycle value together with the expected discount factor, we find the expected ownership cost curve as a function of the cost,

$$c(m_u) = \frac{p + \frac{b}{r - \alpha} \left(1 - \left(\frac{b}{m_u} \right)^{\beta_1 - 1} \right)}{1 - \left(\frac{b}{m_u} \right)^{\beta_1}}. \quad (36)$$

Differentiating with respect to m_u we find the transcendental equation for m_u^* – the value of m_u that minimizes the expected total ownership cost in the presence of stochastic noise,

$$m_u^* = \frac{\beta_1}{\beta_1 - 1} (r - \alpha) p + \frac{\beta_1}{\beta_1 - 1} (r - \alpha) \frac{\frac{b}{r - \alpha} \left(1 - \left(\frac{b}{m_u^*} \right)^{\beta_1 - 1} \right) + p \left(\frac{b}{m_u^*} \right)^{\beta_1}}{1 - \left(\frac{b}{m_u^*} \right)^{\beta_1}}. \quad (37)$$

In the deterministic model, in which $\sigma = 0$, we find the analogous relation,

$$m_u^* = rp + r \frac{\frac{b}{r - \alpha} \left(1 - \left(\frac{b}{m_u^*} \right)^{r/\alpha - 1} \right) + p \left(\frac{b}{m_u^*} \right)^{r/\alpha}}{1 - \left(\frac{b}{m_u^*} \right)^{r/\alpha}}. \quad (38)$$

Note that the eq(38) conveys the same information as eq.(6) since the deterministic case links the replacement age and the O&M cost per utility in a one-to-one manner.

Comparison of eq.(37) and eq.(38) reveal the essential difference concerning the value of waiting. The deterministic case balances the marginal costs and the known savings from delay through a small increment in time. On the other hand, the stochastic case balances the marginal costs and savings from delaying until the O&M costs per utility increase by a small increment. In the stochastic case, the time interval required to increment the O&M costs per utility by a given amount is random.

3 Results: model application to data

We apply the stochastic model developed in the previous sections to the CP-140A Arcturus maritime patrol aircraft. This fleet's homogeneous characteristics affords us a testbed for the model. On the other hand, the CP-140A fleet consists of only three aircraft and thus represents a limited data set. Using data provided by the Cost Factors Manual (CFM) [24], the PERFORMA database [25], and data used by [15], we determine model parameters that allow us to examine the replacement problem from a mean first passage time perspective. In addition, we apply two different utility functions based on availability for discounting purposes.

3.1 Data and model assumptions

Based on the data obtained through the CFM and the PERFORMA database, and provided by [15], we analyze the CP-140A Arcturus for optimal replacement in the presence of stochastic noise. The data contain the annual O&M costs and the average yearly fleet Ao as listed in table 1. We see that the data set contains 13 years of data (1995 - 2007), binned on a yearly basis per aircraft. The acquisition cost of each aircraft was \$79.6 million (1993).

The O&M costs include petroleum, oil, lubricants, engineering services, repairs, overhauls, and sparing costs. Since any amortization costs connected to the fleet do not involve the disbursement of funds, and since usual military activity in the form of salaries or unit support will require funding independent of vehicle age, we do not include costs associated with these effects in O&M. We also assume that the CFM accurately reports the total O&M cost each year. We treat all policy changes on usage as part of the random process.

The model construction looks to determine the optimal replacement time of the fleet, thus we do not consider alternative replacement platforms or new technologies. We stress, that in order to determine if a fleet no longer provides value for money, we must examine the platform's performance in comparison to itself. Comparing new technologies and new capabilities present in replacement alternatives with the current vehicle does not establish a "fair playing field". In essence, we must compare like with like. We do not claim that an alternative replacement comparison does not provide value in making a replacement decision – it most certainly does – but alternative comparisons pose a different problem, more suited to multi-criteria decision analysis (MCDA). The replacement decision arising from a new *required* or *desired* capability presents a fundamentally different problem from replacement arising from economic considerations. Thus, from a purely economic perspective, we must remain indifferent as to replacement choices available.

Based on RAND studies, we take the position that fleet resiliency diminishes with time (e.g. metal fatigue, increased chance of corrosion discoveries), and hence problems triggered by random events – which occur independently of the CP-140A's age – compound. In this

| CP-140A Arcturus Data (fleet size: 3 aircraft) | | |
|--|--------------------------|--------------|
| Year | O&M per Aircraft (\$000) | Fleet Ao (%) |
| 1995 | 2736 | 62.75 |
| 1996 | 2486 | 67.76 |
| 1997 | 2010 | 55.76 |
| 1998 | 2634 | 43.37 |
| 1999 | 3030 | 30.72 |
| 2000 | 2782 | 43.96 |
| 2001 | 3075 | 46.78 |
| 2002 | 3372 | 59.53 |
| 2003 | 3450 | 55.22 |
| 2004 | 3518 | 24.02 |
| 2005 | 4676 | 16.41 |
| 2006 | 3506 | 19.94 |
| 2007 | 5202 | 32.15 |

Table 1: CP-140A Arcturus yearly O&M costs per aircraft and fleet Ao data. Acquisition cost: \$79.6M per aircraft (1993).

sense, the O&M costs experience an exponential random walk with drift. Thus, we apply the mathematical framework of stochastic calculus developed in the Annex to model the CP-140A's O&M cost evolution per utility. Finally, we assume a constant discount rate of 4.40%, which provides a good approximation to a risk-free interest rate in Canada over the period in consideration [15]. Earlier studies [15] showed through a sensitivity analysis that deterministic net present-value calculations remain largely insensitive to moderate changes in the discount rate. Thus, we keep the discount rate fixed throughout the study.

To summarize our model assumptions, we have:

- effects of new technology, modernization, or replacement choice are not considered;
- salaries supporting DND civilian or military personnel are not included in O&M;
- direct squadron support costs are not included in O&M;
- amortization costs are not included;
- time value of money is matched to a savings account at 4.40% fixed rate;
- fleet becomes less resilient to random events with time;
- the utility measure cannot reach unity below 100% Ao; and
- random events occur independently of vehicle life.

3.2 Expected fleet replacement with utility

As a proof of principle example, we first approach the problem of replacement with a utility function obtained from the trapezoid profile that is uniform from 0% to 100% in Ao. In this case, the trapezoid profile reduces to a rectangle. Stated succinctly, the utility obtained from the uniform profile implies that the military expects the fleet to operate between 0% and 100%. In some sense, this utility forms a base case as the utility measure does not bias any interval of Ao (the military remains indifferent to risk throughout the entire Ao range). We will denote this risk indifferent utility as passive and we depict it in figure 9. Notice that in this case, the utility function forms a straight line. Starting from a geometric random walk with drift, we use the stochastic differential equation

$$dm_u = \alpha m_u dt + \sigma m_u dW. \quad (39)$$

For the purposes of numerical analysis, we will find it fruitful to transform eq.(39) by,

$$\tilde{m}_u = \log(m_u). \quad (40)$$

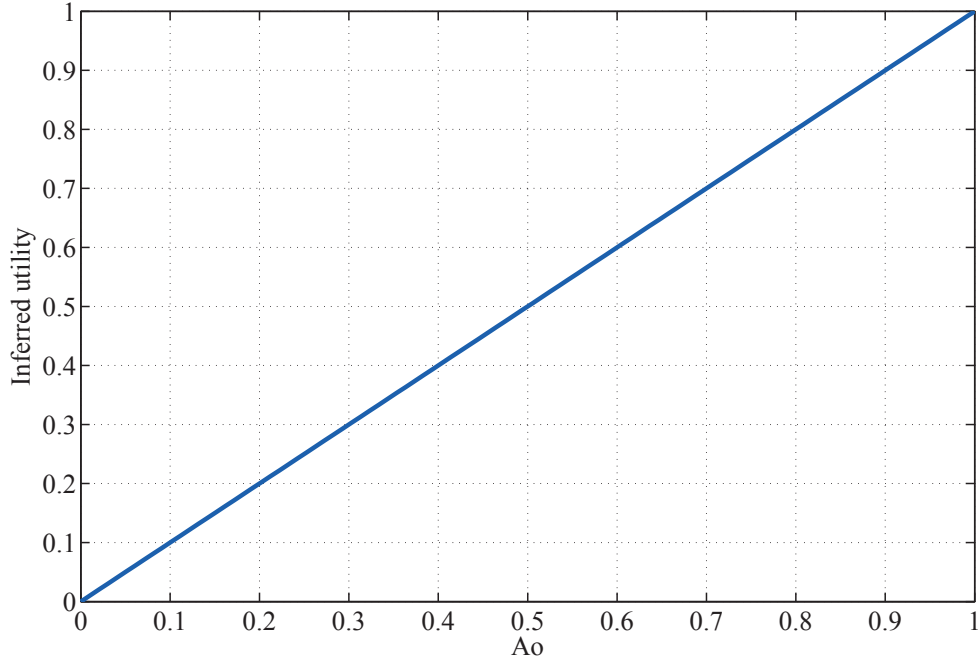


Figure 9: A passive utility function derived from an uniform expectation.

so that Ito's Lemma yields

$$d\tilde{m}_u = \frac{dm_u}{m_u} - \frac{1}{2} \frac{(dm_u)^2}{m_u^2} = (\alpha - (1/2)\sigma^2)dt + \sigma dW. \quad (41)$$

Using the logarithmic form the of eq.(39), we see through the Chapman-Kolmogorov equation, eq.(A.7), and through the Fokker-Planck equation that eq.(41) represents a random walk with drift (no longer a geometric random walk), implying that each increment becomes normally distributed. In the logarithmic space we find the conditional probability

$$p(x_j, t_j | x_i, t_i) = \frac{1}{\sqrt{2\pi\sigma^2(t_j - t_i)}} \exp \left[-\frac{((x_j - x_i) - (\alpha - (1/2)\sigma^2)(t_j - t_i))^2}{(2\sigma^2(t_j - t_i))} \right]. \quad (42)$$

where x_i denotes the logarithmic transformed recorded O&M cost per utility and t_i labels the time. If we examine the CP-140A data on a yearly basis, we can estimate the expected logarithmic annual growth rate $(\alpha - (1/2)\sigma^2)$ and the yearly volatility, σ , using a maximum likelihood technique. Once we obtain the central values and the associated errors for the parameter set, we can test the result for normality as the model demands that each yearly difference follows a stationary Gaussian random process. In particular, the model

yields ⁴,

$$\Delta x_i = x_{i+1} - x_i \sim N(\alpha - (1/2)\sigma^2, \sigma^2) \quad (43)$$

and through the likelihood analysis, we find

$$\hat{\alpha} = 0.2 \pm 0.1 \quad \hat{\sigma} = 0.4 \pm 0.1 \quad (44)$$

The data set contain a small number of data points resulting in only 12 differences. Given eq.(42), the model demands that the yearly differences $\Delta x_i = x_{i+1} - x_i$ generate a Gaussian white noise sequence with mean $(\alpha - (1/2)\sigma^2)$ and with variance σ^2 . Thus, we test the sequence of differences, Δ_i , for normality by examining the autocorrelation function of the data and by using the Portmanteau test, the turning point test, the difference-sign test, and the rank test [26]. If the data significantly fails a number of these tests, our geometric random walk hypothesis will fail to describe the O&M cost per utility process. We begin by constructing the sample autocovariance function, $\gamma(h)$, and the sample autocorrelation function, $\rho(h)$, for the data

$$\gamma(h) = \frac{1}{12} \sum_{i=1}^{12-|h|} (\Delta x_{i+|h|} - \bar{\Delta x})(\Delta x_i - \bar{\Delta x}) \quad (45)$$

$$\rho(h) = \frac{\gamma(h)}{\gamma(0)}. \quad (46)$$

If eq.(42) describes the differences, $\rho(h)$ should show no correlations at lag $h > 0$. At the 95% confidence level, we should find that the sample autocorrelation function lies between $\pm 1.96/\sqrt{12} = 0.58$. Figure 10 demonstrates the result and suggests that, at the level of the autocorrelation function, the hypothesis given by eq.(42) survives. In addition to passing the constraint provided by the 95% confidence level in the sample autocorrelation function, the Portmanteau test demands that the expression

$$Q(h) = 12 \sum_{i=1}^h \rho^2(i) \quad (47)$$

behaves as a χ^2 distribution with h degrees of freedom for Gaussian white noise. Using $\rho(h)$ extracted from the data, we show the $Q(h)$ values in table 2 along with the χ^2 critical values at the 95% level. Our hypothesis survives the test but again we acknowledge the limited data set.

Finally we apply the three remaining tests on our data analysis. The turning point test counts the number of times the data exhibits a change in direction *i.e.*, $\Delta x_{i-1} < \Delta x_i$ and $\Delta x_i > \Delta x_{i+1}$, or $\Delta x_{i-1} > \Delta x_i$ and $\Delta x_i < \Delta x_{i+1}$. In our case, the expected number of turning points for Gaussian white noise is 6 ± 1 while the data exhibits 5. Our result again satisfies

⁴We use \sim to denote “distributed as”.

| Portmanteau Test | | |
|------------------|---------|-------------------------|
| Lag | Q-value | $\chi^2_{crit}(P=0.05)$ |
| 1 | 0.1 | 3.84 |
| 2 | 3.1 | 5.99 |
| 3 | 3.8 | 7.82 |
| 4 | 4.0 | 9.49 |
| 5 | 4.0 | 11.07 |
| 6 | 6.5 | 12.59 |
| 7 | 6.5 | 14.07 |
| 8 | 7.7 | 15.51 |
| 9 | 7.6 | 16.92 |
| 10 | 7.7 | 18.31 |
| 11 | 7.8 | 19.68 |

Table 2: Portmanteau test for normality

the test. The difference test counts the number of times the difference $\Delta x_i - \Delta x_{i-1}$ appears positive. Gaussian white noise with our 12 data points gives the expected result 6 ± 1 , and the data concord with this test with 6 occurrences. In order to test for the possibility of a linear trend in the data, we use the rank test which counts the number of data pairs (i, j) with $\Delta x_j > \Delta x_i$ and with $j > i$. With our data we expect 33 ± 7 such pairs, and we find 35. We display the results of these tests in table 3.

While the data satisfy the statistical tests we applied, thus giving no compelling evidence to reject our hypothesis of a geometric random walk, the limited sample size and the unknown uncertainty in the costing data will not allow us to reject easily other alternative hypotheses. Since the costs evolve in an economic inflationary background under the additional assumption of diminishing aircraft resiliency, we expect that we can capture the process using a geometric random walk. We caution the reader that data must empirically demonstrate geometric random walk behaviour in order to use the model under consideration and, as discussed in the previous section, the stochastic properties of Ao can in principle upset our assumption of a geometric random walk.

Having extracted the estimates for the parameter set from the data with the associated errors, we must now incorporate this information within the model. Recall that on solving eq.(39) and eq.(41), we will obtain the process that yields sample paths. Each sample path is a different realization of the process, and thus we must proceed carefully with our limited knowledge of $\hat{\alpha}$ and $\hat{\sigma}$. Instead of creating classes of sample paths associated with

| Additional Tests | | | |
|------------------|----------------|------------|--------|
| Test | Expected Value | Data Value | Passed |
| Turning Point | 6 ± 1 | 5 | YES |
| Difference | 6 ± 1 | 6 | YES |
| Rank | 33 ± 7 | 35 | YES |

Table 3: Additional statistical tests for normality

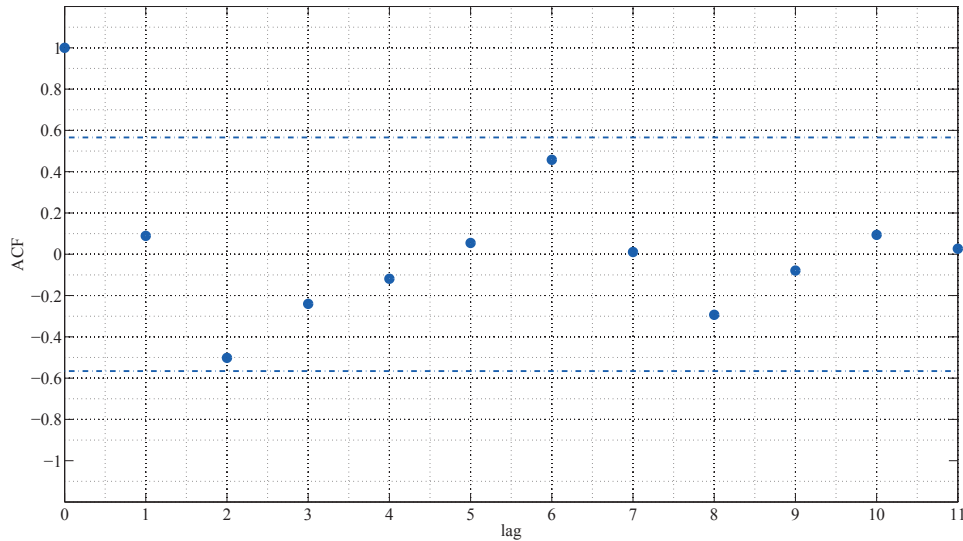


Figure 10: The sample autocorrelation function for differences Δx_j . Note that the data lies within the 95% confidence boundaries denoted by the dashed lines. No correlations exists for lags larger than 0.

varying model parameters, we include the uncertainty in the model parameters through determination of the expected O&M costs per utility value at replacement. By including the uncertainty in the model parameters, the boundary value m_u^* , determined by eq.(37), becomes a region, $m_u^* \pm \Delta m_u^*$, rather than a precise barrier. The level of uncertainty in the model parameters dictates the size of the region. We interpret this region as a critical region for the procurement process or overhaul decision. Once the sample path wanders into the critical region, the model signals fleet replacement/overhaul. In the remainder of the analysis, we assume the maximum likelihood values of the parameter with all the uncertainty embedded in the critical region. Using the CP-140A data with the passive utility function, we find that the critical region at the 95% confidence level arising from the

model parameters becomes

$$\$15.5 \times 10^6 / \text{utility} < m_u^* < \$39.9 \times 10^6 / \text{utility}. \quad (48)$$

We will use the identification $L = \$15.5 \times 10^6 / \text{utility}$ and $U = \$39.9 \times 10^6 / \text{utility}$ in the remainder of the analysis with \tilde{L} and \tilde{U} denoting their logarithmic transformations.

To emphasize the random process under discussion, consider figure 11. In this figure, we see the CP-140A Arcturus data labelled by red points and interpolated with a blue line. The green paths represent alternative scenarios based on the central values for the model parameters obtained from the likelihood analysis. Each green path represents a separate realization of the O&M cost per utility evolution, and the dashed red parabola gives the contour that encloses 95% of all possible paths.

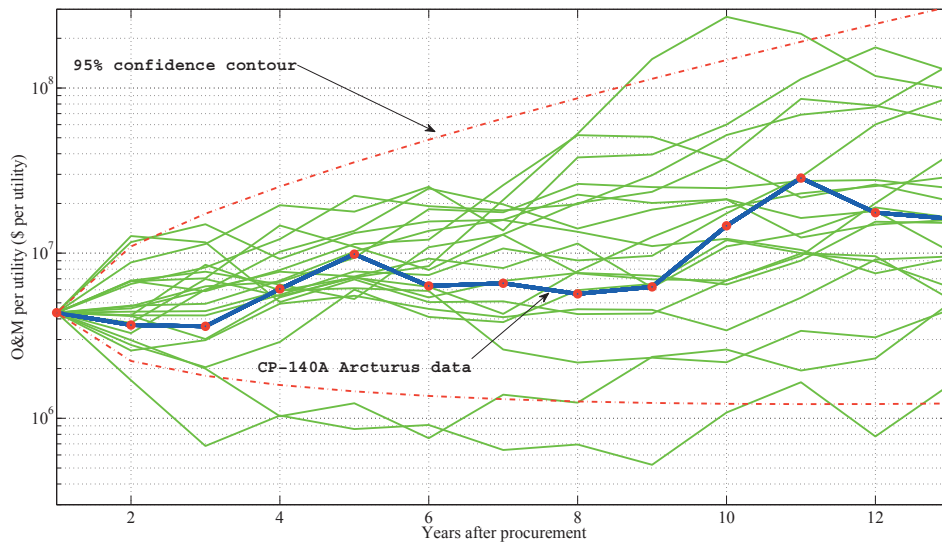


Figure 11: CP-140A Arcturus data superimposed on other possible sample paths generated by the model. The red contour denotes the boundary that contains 95% of all possible sample paths.

The model definition in section 2 considers perfect information on the model parameters. The application of the model to data generates the critical region from model parameter uncertainty. Thus, we can adapt the model in the presence of real data by recognizing that expectation values associated with the critical region represent the crucial information required by the decision-maker. In this context, we will reframe the problem in the language of a mean first passage time and develop the extension with the CP-140A data in mind. We will develop this approach in some detail.

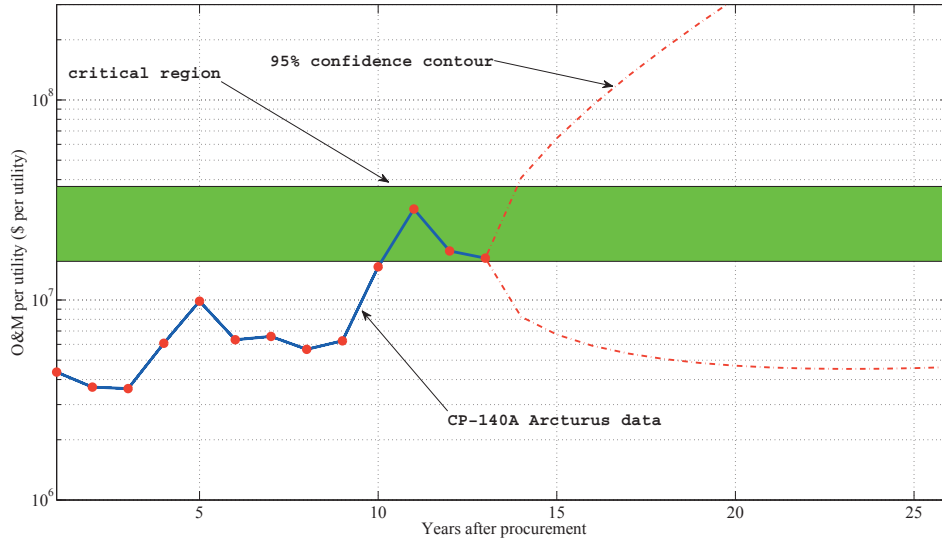


Figure 12: CP-140 Arcturus data with the critical region extracted from the data. Notice that at year 11 the sample path drifted into the critical region only to wander lower in the subsequent time steps.

The backward Fokker-Planck equation affords us the ability to forecast sojourn times of the sample path within a specific region while also permitting us to calculate the probability of exit through a particular boundary. In order to gain a greater understanding of the mean first passage time approach, we will assume a general, time homogeneous, stochastic process obeying the SDE (see Annex for details)

$$dx = A(x)dt + \sqrt{B(x)}dW. \quad (49)$$

We now imagine that the process starts from $x = x_0$ at $t = 0$ with $a \leq x_0 \leq b$. Thus a and b define the interval (a, b) and, assuming that the boundaries constitute an exit, we seek the mean first passage through a particular endpoint. The probability (conditional on the initial conditions) that we find the process within the interval (a, b) at some later time t reads,

$$\text{Prob}(T \geq t) = F(x, t) \equiv \int_a^b dx' p(x', t|x, 0) \quad (50)$$

where T denotes the time that the process leaves the region. We will use eq.(50) directly for forecasting purposes later in this section. Applying the backward Fokker-Planck we find,

$$\frac{\partial F(x, t)}{\partial t} = A(x) \frac{\partial F(x, t)}{\partial x} + \frac{1}{2} B(x) \frac{\partial^2 F(x, t)}{\partial x^2}, \quad (51)$$

and, in light of the initial condition $p(x', 0|x, 0) = \delta(x - x')$, we have,

$$\begin{aligned} F(x, 0) &= 1 \quad a \leq x \leq b \\ &= 0 \quad \text{elsewhere.} \end{aligned} \quad (52)$$

If the process finds itself at either endpoint, we assume that the process immediately exits,

$$F(a, t) = F(b, t) = 0. \quad (53)$$

The function $F(x, t)$ gives the probability that the exit time, T , is larger than the current time t . Thus, the mean first passage time to exit must be given by

$$E(T) \equiv T(x) = - \int_0^\infty dt t \frac{\partial F(x, t)}{\partial t} = \int_0^\infty dt F(x, t). \quad (54)$$

Applying the backward Fokker-Planck equation once more yields the differential equation for $T(x)$

$$A(x) \frac{\partial T(x)}{\partial x} + \frac{1}{2} B(x) \frac{\partial^2 T(x)}{\partial x^2} = -1 \quad (55)$$

with $T(a) = T(b) = 0$. We see that eq.(55) matches the dynamic programming result eq.(18), with the appropriate substitutions for $A(x)$ and $B(x)$. Eq.(55) can readily be extended to the higher moments, $T^n(x)$.

While the solution to eq.(55) gives the mean first passage time, we can also find the overall probability that, given a starting point within the interval (a, b) , that the process will exit through a particular end. We intuitively suspect that if the process starts close to b , the process will exit through b more often than through a . Using the backward Fokker-Planck equation together with the concept of a probability current [18], we find that the probability of eventual exit through a , π_a , given that the process starts at x , obeys the homogeneous differential equation

$$A(x) \frac{\partial \pi_a(x)}{\partial x} + \frac{1}{2} B(x) \frac{\partial^2 \pi_a(x)}{\partial x^2} = 0 \quad (56)$$

with $\pi_a(a) = 1$ and $\pi_a(b) = 0$. The boundary conditions have the immediate interpretation that if the process finds itself at a , it will (almost-surely) exit through a , and if at b , the process will (almost-surely) exit through b . A similar equation exists for $\pi_b(x)$ with the condition

$$\pi_a(x) + \pi_b(x) = 1. \quad (57)$$

Based on the solution to eq.(15) or with the use of the backward Fokker-Planck equation, eq.(A.9), and eq.(55) we find (in the logarithmic space) the expectation time, $a(\tilde{m}_u)$, for the CP-140A sample path to remain inside a bounded interval $\tilde{m} \in [X, Y]$, satisfies

$$k_1 \frac{d^2 a}{d\tilde{m}_u^2} + k_2 \frac{da}{d\tilde{m}_u} = -1 \quad (58)$$

where $k_1 = (1/2)\sigma^2 = 0.08$ and $k_2 = \alpha - (1/2)\sigma^2 = 0.12$ are extracted from the CP-140A data. The solution to eq.(58) has the form,

$$a(\tilde{m}_u) = A \exp\left(-\frac{k_2}{k_1}\tilde{m}_u\right) - \frac{\tilde{m}_u}{k_2} + B \quad (59)$$

where A and B denote arbitrary constants determined by the boundaries X and Y . Since we are interested in the average time for the sample path to remain below the lower boundary of the critical region, \tilde{L} , the interval, $[X, Y]$, that we require for eq.(58) becomes $\tilde{m}_u \in (-\infty, \tilde{L}]$ (recall that since we are in logarithmic space, $-\infty$ corresponds to the absorbing point of the geometric random walk). With these boundaries, we find that

$$A = 0 \quad B = \frac{\tilde{L}}{k_2}, \quad (60)$$

leading to the replacement expectation time for entering or surpassing the critical region with starting point \tilde{m}_{u0} ,

$$a(\tilde{m}_{u0}) = -\frac{\tilde{m}_{u0}}{k_2} + \frac{\tilde{L}}{k_2}. \quad (61)$$

Eq.(61) allows us to forecast by giving us the expectation of entering the critical region from any time step using the current year O&M costs per utility $\tilde{m}_{u\text{current}} = \tilde{m}_{u0}$. Given the first year of data, we find the model yields an expectation time for fleet replacement of 11 years.

Returning to normal dollar per utility space, we see that eq.(61) matches the expected age of replacement obtained from eq.(20) through dynamic programming methods. Using a Monte Carlo approach for the CP-140A, we show the distribution for the replacement expectation time in figure 13. Note that the wide variance around the 11 year expectation time, (6, 21) years at the 60% confidence level, reflects the noise-dominated process. An analytic expression for this distribution can be obtained by integrating the moment extensions of eq.(55). Note that while the model yields an expectation time of 11 years, the result depends crucially on the utility function choice. If we ignore the utility function (or equivalently, turn the trapezoid profile into a Dirac-delta function located at 0% Ao), the expectation time for replacement/overhaul jumps by more than 100% to 23 years. We stress that consensus on the subjective utility function must be established prior to the model's application.

Once \tilde{m} has diffused into the critical region, we can determine the expected sojourn time as well as the probability that the processes exits through the upper boundary, \tilde{U} , or the lower boundary \tilde{L} . From a forecasting standpoint, this information will help establish the chance that the platform will improve or worsen in the near future. First, we imagine that the process wanders into the critical region $[\tilde{L}, \tilde{U}]$. The probability that the process wanders through \tilde{U} before \tilde{L} satisfies the differential equation

$$k_1 \frac{d^2 \pi_U(\tilde{m}_u)}{d\tilde{m}_u^2} + k_2 \frac{d\pi_U(\tilde{m}_u)}{d\tilde{m}_u} = 0. \quad (62)$$

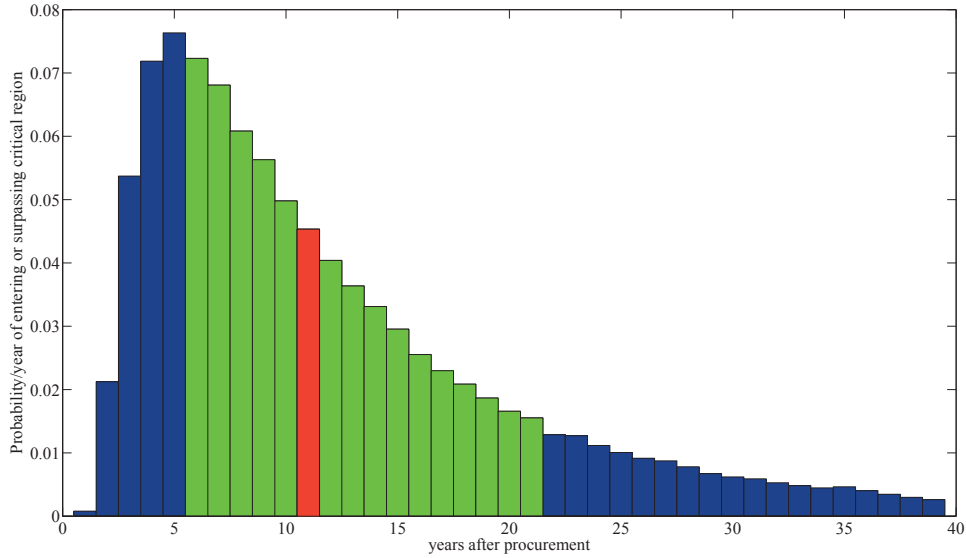


Figure 13: The probability distribution for the replacement time. The red bar denotes the expected replacement time, while the green bars show the 60% confidence region. Again, we have used the passive utility function.

with $\pi_{\tilde{U}}(\tilde{U}) = 1$ and $\pi_{\tilde{U}}(L) = 0$. Solving eq.(62), we find,

$$\pi_{\tilde{U}}(\tilde{m}_u) = \frac{e^{-\frac{k_2}{k_1}\tilde{m}_u} - e^{-\frac{k_2}{k_1}\tilde{L}}}{e^{-\frac{k_2}{k_1}\tilde{U}} - e^{-\frac{k_2}{k_1}\tilde{L}}} \quad (63)$$

$$\pi_{\tilde{L}}(\tilde{m}_u) = 1 - \frac{e^{-\frac{k_2}{k_1}\tilde{m}_u} - e^{-\frac{k_2}{k_1}\tilde{L}}}{e^{-\frac{k_2}{k_1}\tilde{U}} - e^{-\frac{k_2}{k_1}\tilde{L}}}. \quad (64)$$

Note that a similar equation holds for the probability that the path diffuses through L before U . Figure 14 and figure 15 show the probability of diffusing through the lower and upper boundaries as a function of the position within the critical region. Also, note that we have $k_1, k_2 > 0$ in the above analysis.⁵

If the process wanders into the critical region, $\tilde{m}_u \in (L, U)$, we can obtain the expected

⁵Alternative solutions exist if we relax the positive-definite conditions on k_1 and k_2 , but we must ensure that the solution is sensible. From a technical standpoint, the process we consider is a submartingale – that is, the process drifts upward in time. If the system has zero drift (a martingale process) or negative drift (a supermartingale process), the expectation time to the critical region from below will not exist. We caution that in extracting the parameters α and σ from the data, we must ensure that we obtain a submartingale process to apply this model.

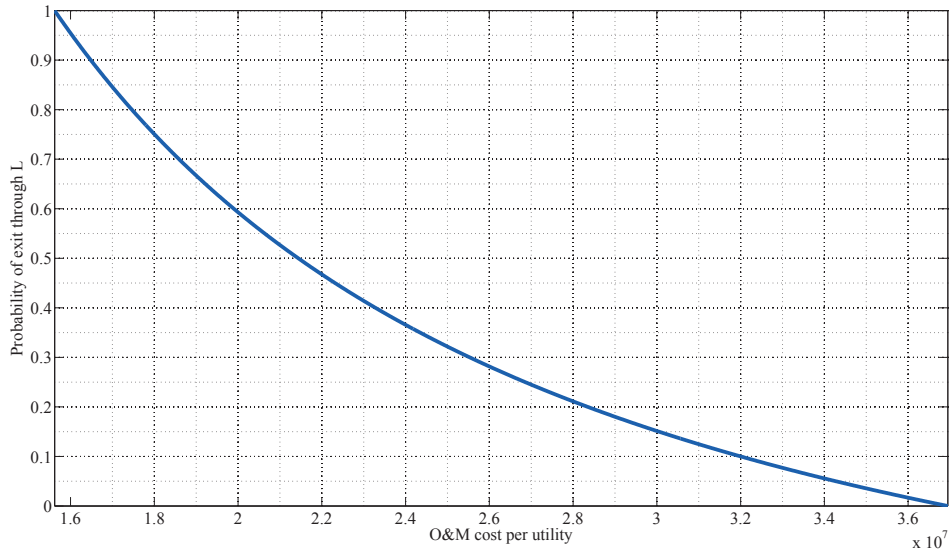


Figure 14: The probability that the CP-140A path, with the passive utility discount, will diffuse through the lower boundary, $L = \$15.6$ million per utility, before the upper boundary, $U = \$36.9$ million per utility, as a function of position inside the critical region.

sojourn time within this region by solving eq.(55) with the boundaries L and U ,

$$T(\tilde{m}_u) = \frac{1}{k_2} \left[\frac{(\tilde{U} - \tilde{L}) \left(e^{\frac{-k_2}{k_1} \tilde{U}} - e^{\frac{-k_2}{k_1} \tilde{m}_u} \right)}{\left(e^{\frac{-k_2}{k_1} \tilde{L}} - e^{\frac{-k_2}{k_1} \tilde{U}} \right)} - \tilde{m}_u + \tilde{U} \right] \quad (65)$$

Using eq.(55) and eq.(65) together, we can quantify the full range of expectation times required for fleet replacement. In particular, the expected sojourn time, calculated from the current year position within (\tilde{L}, \tilde{U}) , yields the expected time the process remains confined within the critical region, and the mean first passage time gives the expected time for first entry. Notice that there is a probability that the fleet will drift out of the critical region in a favorable fashion. Again, we see that the model places a value on the capacity to wait and includes the possibility of improvement within the expectation time calculation. In figure 12, we see that the third last data point for the CP-140A lies inside the critical region. Based on eq.(62) and eq.(65), we find that the expected sojourn time in the region from this CP-140A data point is 0.8 years, and that the probability of exit through the \tilde{U} and \tilde{L} is 0.8 and 0.2 respectively. Thus, we see that the CP-140A fleet received a favourable bump, knocking the sample path below the lower boundary.

In conjunction with eq.(65), we can compute the probability, as a function of time, t , that

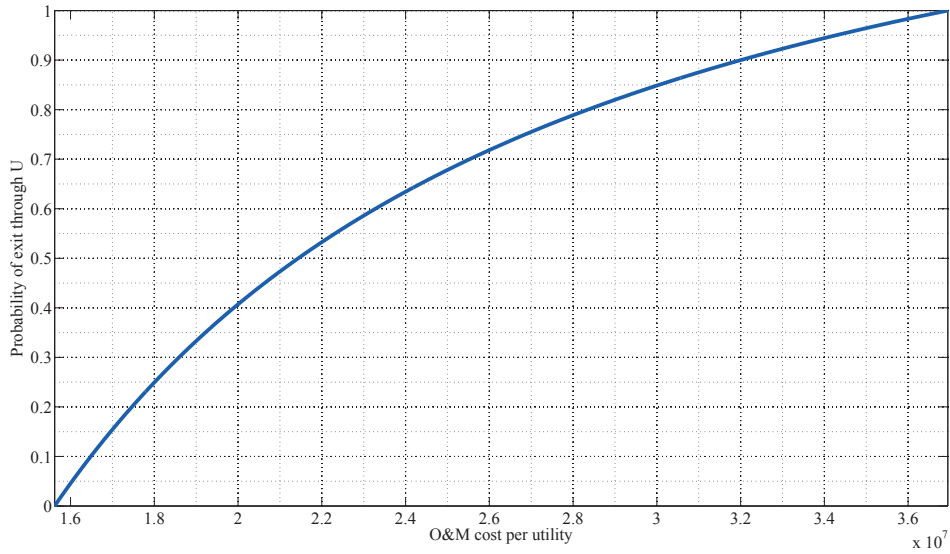


Figure 15: The probability that the CP-140A path will diffuse through the upper boundary $U = \$36.9$ million per utility, before the lower boundary, $L = \$15.6$ million per utility, as a function of position inside the critical region.

the process continues to remain below the critical region at t . Assuming that the process has not previously entered the critical region, $\tilde{m} \in (-\infty, L)$, we integrate eq.(50) to find the probability,

$$P(t) = \frac{1}{2} \left(1 - \operatorname{erf} \left(\frac{(\tilde{L} - \tilde{m}_u) - k_2 t}{\sqrt{2\sigma^2 t}} \right) \right) \quad (66)$$

where \tilde{m}_u denotes the current year position and $\operatorname{erf}(\cdot)$ denotes the error function. Eq.(66) provides forecasting capabilities – from any time step we can compute the probability that the process will enter the critical region based on a given time horizon. Figure 16 gives the probability that the CP-140A sample path reaches the lower boundary of the critical region L , by time t measured from the time of initial procurement. We see in figure 16 that by year 12, 50% of the possible sample paths will cross the lower boundary of the critical region.

3.3 Non-passive utility

Thus far, we have demonstrated our results using the passive utility function, $U(Ao) = Ao$. For completeness, we present a more refined approach that uses a different expected utility function. We reproduce figures 11 to 16 with a non-passive utility function derived from the expectation interval 60% – 75% with the solution given by figure 8. Note that the utility function in figure 8 penalizes the lack of availability in the low range more than the linear utility function used previously. Again we allow the trapezoid profile to run

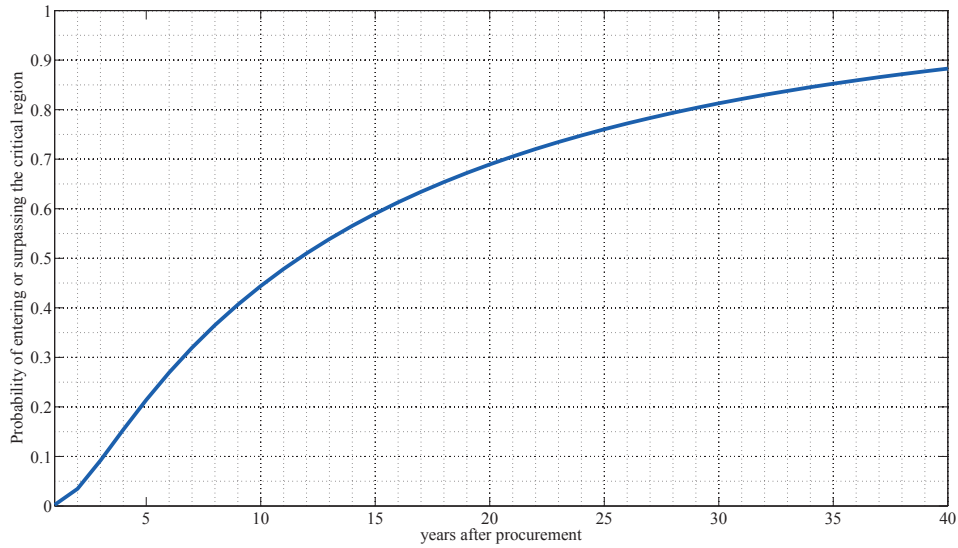


Figure 16: The probability as a function of time, t , that the CP-140A reaches the critical region starting from the initial procurement data using the passive utility discount.

from 0% to 100% in Ao. The following result will give a lower bound on the expected replacement/overhaul decision time for utility functions in the 60% – 75% class.

Figures 17 to 22 demonstrate that the model calls for an earlier decision on CP-140A fleet when we use the new choice of utility 8. We should expect this result since the recorded Ao only reached the expected Ao range twice (1995, 1996). In particular, note that the last few data points of figure 18 experience a much greater upward shift as the result of declining availability. Repeating our previous analysis with the new utility function, we find the model parameters

$$\hat{\alpha} = 0.4 \pm 0.2 \quad \hat{\sigma} = 0.7 \pm 0.2 \quad (67)$$

with critical region

$$\text{\$}23.5 \times 10^6 / \text{utility} \leq m_u^* \leq \text{\$}61.1 \times 10^6 / \text{utility}. \quad (68)$$

Applying the tests for normality, we once again find no compelling evidence to reject the hypothesis of Gaussian increments. Our new utility choice gives an expectation time for replacement of 9 years with the 60% confidence boundary of (4,20) years and that over 50% of all sample paths will drift into the new critical region by year 10. Notice in figure 18 that the critical region has changed as a result of the new model parameters. We see that the utility choice can have a large impact on the replacement decision.

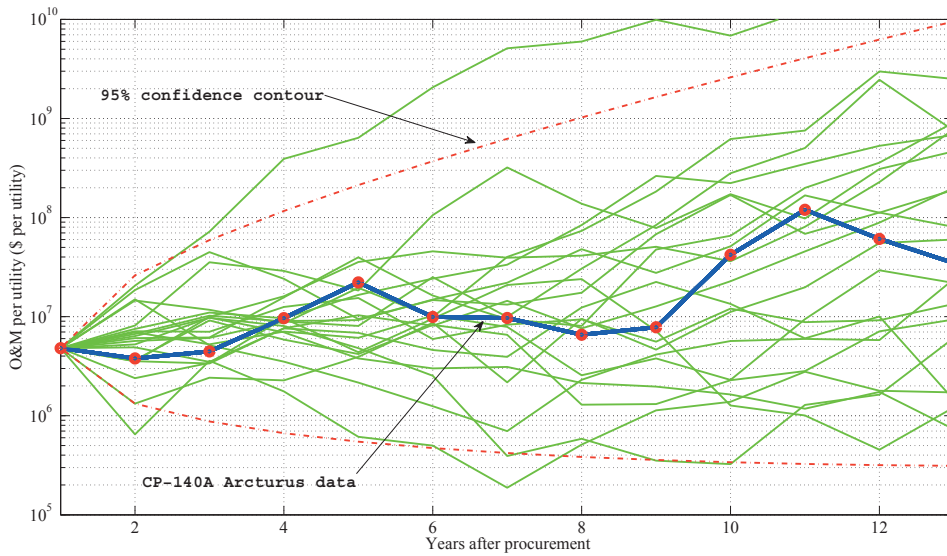


Figure 17: CP-140A Arcturus data superimposed on other possible sample paths generated by the model with the utility function given in figure 8. The red contour denotes the boundary that contains 95% of all possible sample paths.

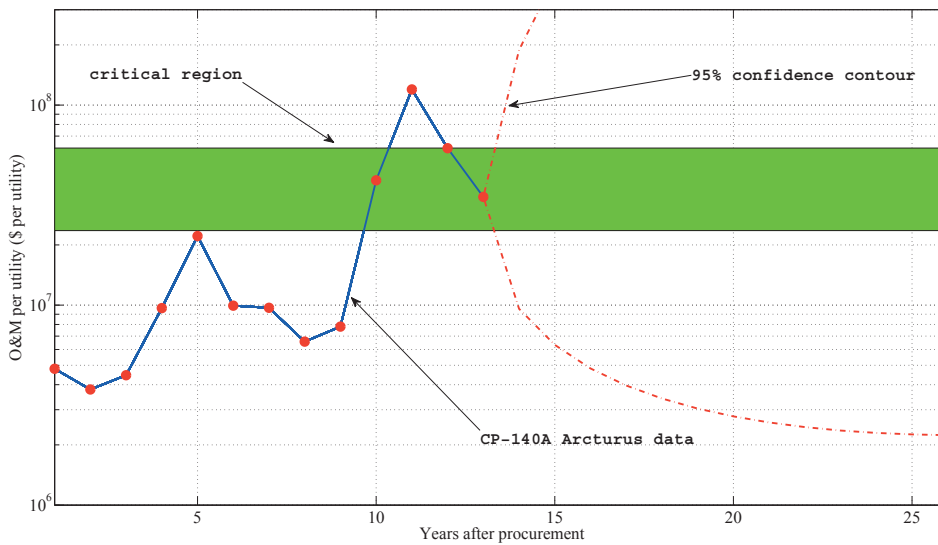


Figure 18: CP-140 Arcturus data with the critical region extracted from the data. Notice that at year 11 the sample path drifted through the critical region only to wander lower in the subsequent time steps.

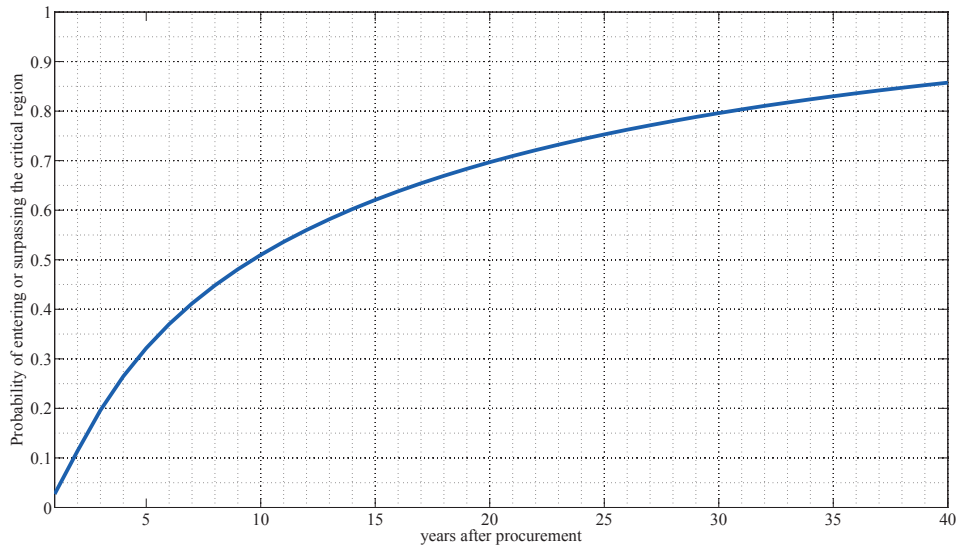


Figure 19: The probability as a function of time, t , that the CP-140A reaches the critical region starting from the initial procurement data using the utility function given in figure 8.

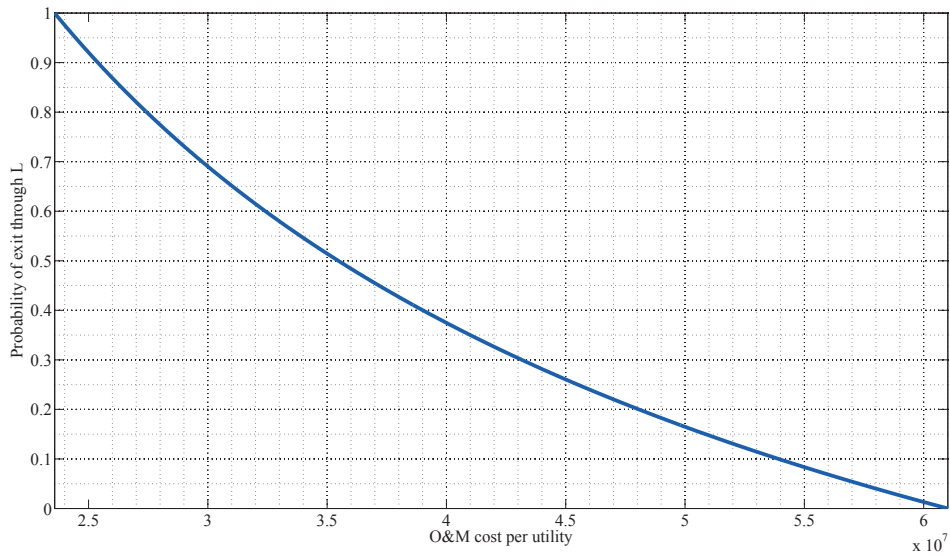


Figure 20: The probability that the CP-140A path will diffuse through the lower boundary, $L = \$23.6$ million per utility, before the upper boundary, $U = \$61.0$ million per utility as a function of position inside the critical region, using the utility function in figure 8.

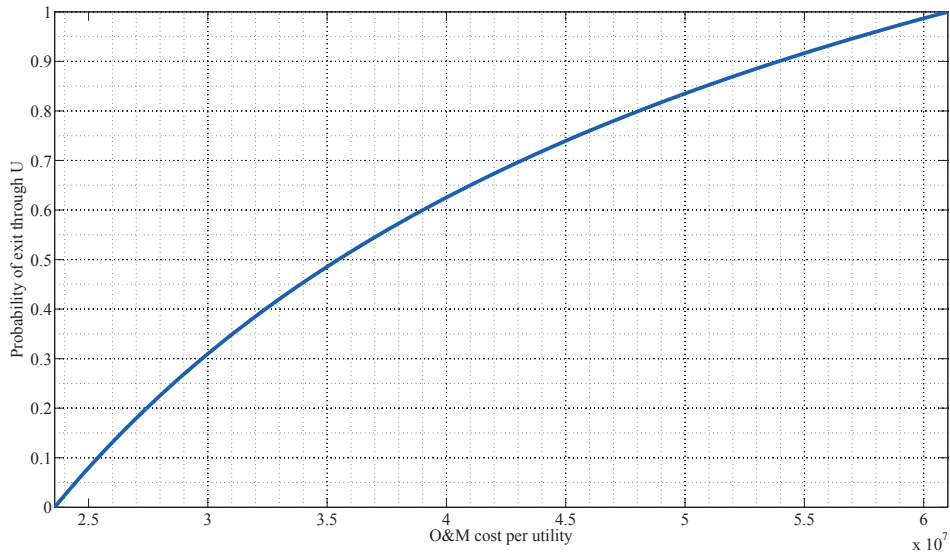


Figure 21: The probability that the CP-140A path will diffuse through the upper boundary $U = \$61.0$ million per utility, before the lower boundary, $L = \$23.6$ million per utility, as a function of position inside the critical region, using the utility function in figure 8.

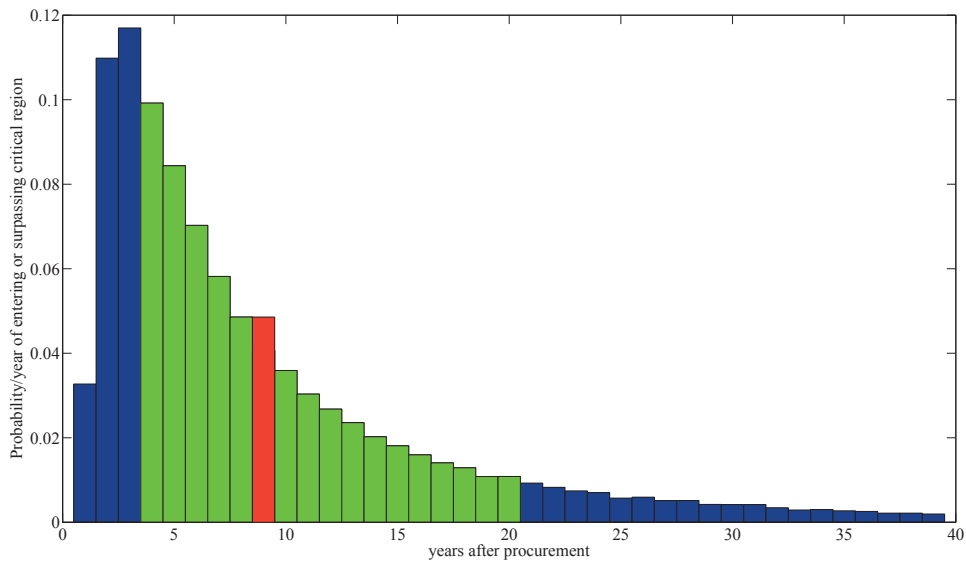


Figure 22: The probability distribution for the replacement time with the utility function given in figure 8. The red bar denotes the expected replacement time, while the green bars show the 60% confidence region

4 Discussion and conclusions

The stochastic model developed for the CP-140A Arcturus fleet replacement problem attempts to capture the random features that systems exhibit over long periods of time. In this sense, the model treats the fleet not unlike the problem of pricing a financial derivative. The model extracts a critical region from the total expected ownership cost per utility curve, which delineates the replacement interval. We note that replacement under uncertainty contains nonintuitive features, such as the lengthening of the expected time of replacement, when compared to the deterministic approach. Analogous to the forest harvester's problem [19], uncertainty plays a large role in determining the optimal replacement interval.

This model indicates that under a passive utility function obtained from the trapezoid profile that extends from 0% to 100%:

- The CP-140A entered the critical region for decision at year 11 (calendar year 2006), and that the CP-140A sample path has an expectation time to reach the critical region of 11 years (calendar year 2006) after procurement. The sample path has not left the critical region and the 60% confidence interval around the expectation is 6 to 21 years (2001 – 2017).
- If we ignore the utility function (or equivalently, turn the trapezoid profile into a Dirac-delta function located at 0% Ao), the expectation time for replacement/overhaul jumps by more than 100% to 23 years.
- The passive utility function represents an unbiased expectation of Ao, but always penalizes the fleet for Ao below 100%. Thus, the result represents a lower bound on all possible passive utility functions.
- Under the assumption that the passive utility function captures the CP-140A fleet's performance expectation, the model calls for the initiation of a replacement/overhaul decision process.

We caution the reader that we should not view the critical region solely in terms of fleet replacement. The critical region simply denotes the place in O&M per utility space where expected total ownership costs begin to realize an expected incurred marginal cost per utility. We imagine that several external variables, such as queueing problems or sparing issues, can create an adverse growth environment and corrections in these areas might radically drive the sample path away from the critical region in a non-stochastic manner. Furthermore, we might find it advantageous to undertake a “reset-the-clock” overhaul rather than acquiring a new fleet once the sample path has drifted into the critical region. Ideally, we see the stochastic model presented in this paper used in conjunction with other decision tools.

While the model treats all random events as a diffusion process, random events exist that do not follow this pattern. The fleet may be subject to processes that force large discrete upward jumps in the the O&M cost per utility path. In particular, we might view certain types of modernization programs as a jump process. The current model does not include this type of effect. In addition to jump processes, we also imagine that the underlying growth function more generally might exhibit non-exponential growth. In this case, the deterministic part of the model will change, leaving us with a different Fokker-Planck equation than the one derived in our analysis. Clearly, jump processes and non-exponential growth functions represent an area for further investigation, but we will require data of sufficient quality to extract these secondary features.

Perhaps the greatest area for further research lies with the stochastic behaviour of the utility discount. Firstly, we caution the reader that the utility function plays a significant role in establishing the expectation time to reach the critical region. The expectation time can move by more than 100% by ignoring utility completely. While the trapezoid profile represents a useful construct and was developed with input from DGAEPM staff [23], other profiles or utility functions may be more appropriate and will in general be fleet specific. Furthermore, we have allowed the domain of the trapezoid profile to extend from 0% to 100% in Ao. A more realistic approach would involve establishing an upper bound in Ao to restrict the profile. We see this as an opportunity for further research. Secondly, we have treated the O&M cost per utility as a single stochastic variable. The statistical tests we performed on the data gave us no compelling reason to abandon this approach. In reality, the O&M costs and the utility discount both evolve stochastically. In a previous study that examined the availability of the CH-149, it was learned [27] that availability behaved as a stochastic mean reverting process. Thus, we can imagine the fleet replacement/overhaul problem as a coupled system of stochastic differential equations with O&M cost following a geometric random walk, and the discount utility tracking a mean reverting process (*e.g.*, an Ornstein-Uhlenbeck process with boundaries or a GARCH-type model). In addition, we might advance the model by using a stochastic interest rate with an appropriate industry specific military deflator. Finally, if a wealth of data exists for certain platforms, we can imagine stochastically evolving the volatility parameter itself. We view this area of research as an exciting possibility.

Operational tempo, unforeseen engineering and maintenance problems, and budgeting processes all factor into the evolution of O&M costs of vehicle fleets. Separating specific variables that directly relate to age from other effects presents a daunting task. By treating the problem stochastically under the assumption that fleet resiliency diminishes with time, we can not only predict a probability envelope for the growing costs, but we can also determine the critical time to consider fleet replacement. Most importantly, the stochastic approach implicitly attaches a value to the capacity to delay in making the replacement decision – as more information becomes available to the decision makers, better choices can be made. Deterministic methods that focus only on marginal costs ignore this important feature. The model we construct balances economic considerations, uncertainty, and fleet

utility in establishing a replacement time. We see the application of stochastic models – similar to the type discussed in this study – to a wide variety of military fleets as fertile ground for future operations research.

References

- [1] Department of National Defence, Canada's Airforce: The CH-124 Sea King http://www.airforce.forces.gc.ca/site/equip/ch124/specs_e.asp .
- [2] R.E. Johnson, Forecasting the Maintenance Manpower Needs of the Depot System Santa Monica Calif.: RAND, RM-3163-PR (June 1962).
- [3] J.R. Nelson, Life Cycle Analysis of Aircraft Turbine Engines Santa Monica Calif.: RAND, R-2103-AF (1977).
- [4] K.E. Marks, R.W. Hess, Estimating Aircraft Depot Maintenance Costs, Santa Monica, CA: RAND R-2731-PA&E (July 1981).
- [5] T. Ramsey, C. French, and K. R. Sperry, Aircraft Maintenance Trend Analysis briefing, Oklahoma City ALC, and Boeing (1998).
- [6] G. Hildebrandt, and M. Sze, An Estimation of USAF Aircraft Operating and Support Cost Relations, Santa Monica Calif.: RAND, N-3062-ACQ (May 1990).
- [7] M. Dixon, The Costs of Aging Aircraft: Insights from Commercial Aviation Pardee RAND Graduate School (2005).
- [8] J. Johnson, Age Impacts on Operating and Support Costs: Navy Aircraft Age Analysis Methodology Patuxent River MD: Naval Aviation Maintenance Office (August 1993).
- [9] L. Stoll, and S. Davis, Aircraft Age Impact on Individual Operating and Support Cost Elements, Patuxent River MD: Naval Aviation Maintenance Office (July 1993).
- [10] P. Francis, and G. Shaw, Effect of Aircraft Age on Maintenance Costs, briefing, Center for Naval Analyses, Alexandria VA (2000).
- [11] J. Jondrow, R.P. Toast, M. Ye, J. Hall, R.L. Kirk, L.J. Junor, P. J. Francis, G. B. Shaw, D.E. Stanford, and B.H. Measell, Support Costs and Aging Aircraft: Implications for Budgeting and Procurement, CNA Corporation (2002).
- [12] G.T. Kiely, The Effects of Aging on the Costs of Maintaining Military Equipment Washington DC: Congressional Budget Office (2001).
- [13] R.A. Pyles, Aging Aircraft: USAF Workload and Material Consumption Life Cycle Patterns Santa Monica Calif: RAND MR-1641 (2003).
- [14] E.G. Keating, M. Dixon, Investigating Optimal Replacement of Aging Air Force Systems Santa Monica, CA: RAND MR-1763-AF (2003).

- [15] A Sokri, Forecasting the Life Cycle Costs of Military Equipment with Application to the CP-140A Arcturus DRDC CORA (in preparation).
- [16] V.A. Greenfield, and D.M. Persselin, An Economic Framework for Evaluating military Aircraft Replacement, Santa Monica, CA: RAND MR-1489-AF (2002).
- [17] V.A. Greenfield, and D.M. Persselin, How Old is Too Old? An Economic Approach to Replacing Military Aircraft, Defence and Peace Economics **14(5)** (2003), 357-368.
- [18] C.W. Gardiner, Handbook of Stochastic Methods, 3rd Ed. Springer (2003).
- [19] M. Faustamnn, Calculation of the Value which Forest Land and Immature Stands Possess for Forestry Allegmeine Forst- und jagd-Zeitung (1849).
- [20] A.K.S. Jardine, and A. H. C. Tsang, Maintenance, Replacement, and Reliability: Theory and Applications CRC press (Talyor & Francis Group) (2006).
- [21] A.K. Dixit, and R.S. Pindyck, Investment Under Uncertainty Princeton University Press (1993).
- [22] Colonel R. Foster, COS DGAEPM, Private communication (October 2, 2008).
- [23] Major P. Appell, DGAEPM staff Private communication (November 4, 2008).
- [24] National Defence (1994-2007), Cost Factors Manual, Government of Canada, Ottawa.
- [25] InnoVision Consulting Inc. AEPM PERFORMA, DV6000.4000.6052.
- [26] P.J. Brockwell, and R.A. Davis, Introduction to Time Series Springer (2001).
- [27] R. Pall, On Forecasting the Availability of the CH149 Cormorant Fleet DRDC CORA TR 2007-20 (December 2007).

Annex A: Stochastic differential equations

A.1 Motivation

We will begin with a semi-heuristic approach that follows Langevin's solution to Brownian motion in order to gain an intuitive understanding of the theory behind differential equations extended to systems that include noise. We imagine a first order differential equation to which we add an "extremely irregular and rapidly fluctuating random term", $\xi(t)$ with known functions, $a(x,t)$ and $b(x,t)$,

$$\frac{dx}{dt} = a(x,t) + b(x,t)\xi(t). \quad (\text{A.1})$$

By an "extremely irregular and rapidly fluctuating random term", we mean that $\xi(t)$ is statistically independent of $\xi(t')$ for $t \neq t'$ with the condition

$$E(\xi(t)) = 0 \quad (\text{A.2})$$

$$E(\xi(t)\xi(t')) = \delta(t-t'). \quad (\text{A.3})$$

Eq.(A.3) satisfies the absence of correlation at different times, but causes $\xi(t)$ to suffer from an infinite variance. In this sense, the function $\xi(t)$ will serve as a source of idealized "white noise" added to the deterministic part of eq.(A.1). On closer inspection we see that the eq.(A.1) contains a serious pathology (in addition to the infinite variance). The sample paths that we imagine $x(t)$ following, while continuous, must intuitively change direction sharply since the term $\xi(t)$ rapidly and randomly alters the direction of the path. In fact, it can be shown (see for example [18]) that such systems are (almost-surely) everywhere non-differentiable. Thus eq.(A.1) cannot represent a differential equation in the usual sense. On the other hand, we might expect that the fluctuating term $\xi(t)$ remains integrable even if it cannot be differentiated. Thus we imagine that

$$u(t) = \int_0^t dt' \xi(t') \quad (\text{A.4})$$

makes sense. If we impose usual integrability conditions, since $u(t)$ is continuous, we find

$$\begin{aligned} u(t') &= \int_0^t ds \xi(s) + \int_t^{t'} ds \xi(s) \\ &= \lim_{\varepsilon \rightarrow 0} \int_0^{t-\varepsilon} ds \xi(s) + \int_t^{t'} ds \xi(s). \end{aligned} \quad (\text{A.5})$$

Recall that $\xi(t)$ remains independent at different times, which implies that $\xi(s)$ in the first integral above remains independent of $\xi(s)$ in the second integral. Thus, by continuity, we have statistical independence between $u(t)$ and $u(t') - u(t)$. Furthermore, we also find that $u(t') - u(t)$ and $u(t'')$ remain independent for $t'' < t$. Probabilistically, $u(t')$ becomes fully

determined by $u(t)$ and not by any past values. Thus, we learn that $u(t)$ describes a Markov process.

Before we investigate the proper meaning of eq.(A.1) in light of the Markov nature of eq.(A.5), we need to develop the formalism of Markov processes with continuous sample paths. If we denote $p(x, t + \Delta t | z, t)$ as the conditional probability of the path moving to x at time $t + \Delta t$ from z at t , continuous processes require the existence of the following limits (see for example [18]):

$$\begin{aligned} \lim_{\Delta t \rightarrow 0} \frac{1}{\Delta t} p(x, t + \Delta t | z, t) &= W(x | z, t) \\ \lim_{\Delta t \rightarrow 0} \frac{1}{\Delta t} \int_{|x-z| < \varepsilon} dx (x_i - z_i) p(x, t + \Delta t | z, t) &= A_i(z, t) + \mathcal{O}(\varepsilon) \\ \lim_{\Delta t \rightarrow 0} \frac{1}{\Delta t} \int_{|x-z| < \varepsilon} dx (x_i - z_i)(x_j - z_j) p(x, t + \Delta t | z, t) &= B_{ij}(z, t) + \mathcal{O}(\varepsilon) \end{aligned} \quad (\text{A.6})$$

By considering an arbitrary twice-differentiable function, $f(z)$, with the use of eqs.(A.6), the expression $\partial_t \int dx f(x) p(x, t | y, t')$ can be used to show that the probability distribution satisfies the Chapman-Kolmogorov equation,

$$\begin{aligned} \frac{\partial p(z, t | y, t')}{\partial t} &= - \frac{\partial}{\partial z_i} (A_i(z, t) p(z, t | y, t')) + \frac{1}{2} \frac{\partial^2}{\partial z_i \partial z_j} (B_{ij}(z, t) p(z, t | y, t')) \\ &\quad + \int dx (W(z | x, t) p(x, t | y, t') - W(x | z, t) p(z, t | y, t')). \end{aligned} \quad (\text{A.7})$$

Each term in eq.(A.7) has a special significance: $A_i(z, t)$ gives the system a deterministic drift; $B_{ij}(z, t)$ determines the amount of diffusion in the system; and $W(z | x, t)$ triggers discrete jumps. In our model construction, we ignore the possibility of $W(z | x, t)$ terms, however, in the section 4 we discuss the potential of including such terms as model extensions.

Our basic starting point for developing a mathematical model of optimal replacement centers on the partial differential equation for a drift-diffusion process, namely,

$$\frac{\partial p(z, t | y, t')}{\partial t} = - \frac{\partial}{\partial z_i} (A_i(z, t) p(z, t | y, t')) + \frac{1}{2} \frac{\partial^2}{\partial z_i \partial z_j} (B_{ij}(z, t) p(z, t | y, t')). \quad (\text{A.8})$$

In the physics literature, eq.(A.8) is often called the Fokker-Planck equation, and within this context, we will develop its connection to stochastic differential equations (SDE). We should note that the formalism thus far takes the approach of forward time – that is, we seek a differential equation that yields the forward time evolution of the probability distribution. The forward time approach requires that we define initial conditions for the probability distribution and, from the perspective of a physical or financial system, seems intuitively obvious. On the other hand, we can couch the problem in a backward sense by first defining a set of final conditions and seeking a differential equation that yields the backward

time evolution. This approach requires that we hold (z, t) fixed in eq.(A.8) and yields the backward Fokker-Planck equation

$$\frac{\partial p(z, t|y, t')}{\partial t'} = -A_i(y, t') \frac{\partial}{\partial y_i} p(z, t|y, t') - \frac{1}{2} B_{ij}(y, t) \frac{\partial^2}{\partial y_i \partial y_j} p(z, t|y, t'). \quad (\text{A.9})$$

The analysis of mean first passage time problems lend themselves to the backward Fokker-Planck equation since we can readily frame the problem from a final condition perspective.

Returning to eq.(A.5), we see that

$$\text{E}(u(t + \Delta t) - u_o) = \text{E}\left(\int_t^{t+\Delta t} ds \xi(s)\right) = 0 \quad (\text{A.10})$$

and

$$\begin{aligned} \text{E}\left([u(t + \Delta t) - u_o]^2\right) &= \int_t^{t+\Delta t} ds \int_t^{t+\Delta t} ds' \text{E}(\xi(s)\xi(s')) \\ &= \int_t^{t+\Delta t} ds \int_t^{t+\Delta t} ds' \delta(s - s') = \Delta t. \end{aligned} \quad (\text{A.11})$$

The expressions eq.(A.10) and eq.(A.11) yield the Fokker-Planck coefficients

$$A(u_o, t) = \lim_{\Delta t \rightarrow 0} \frac{\text{E}(u(t + \Delta t) - u_o)}{\Delta t} = 0 \quad (\text{A.12})$$

$$B(u_o, t) = \lim_{\Delta t \rightarrow 0} \frac{\text{E}\left([u(t + \Delta t) - u_o]^2\right)}{\Delta t} = 1. \quad (\text{A.13})$$

Thus, $u(t)$ follows a pure Markov diffusion process – the expectation of $u(t)$ for $t > t'$ is simply $u(t')$. The diffusion process represented by $A(u_o, t) = 0$ and $B(u_o, t) = 1$ yields the Fokker-Planck equation,

$$\frac{\partial p(w, t|w_0, t_0)}{\partial t} = -\frac{1}{2} \frac{\partial^2}{\partial z_i \partial z_j} (p(z, t|y, t')) \quad (\text{A.14})$$

with solution

$$p(w, t|w_0, t_0) = \frac{1}{\sqrt{2\pi(t-t_0)}} \exp\left[-\frac{(w-w_0)^2}{2(t-t_0)}\right]. \quad (\text{A.15})$$

We see that the process – referred to as a Wiener process in the mathematics literature – yields a Gaussian distribution with

$$\text{E}(W(t)) = w_0 \quad (\text{A.16})$$

$$\text{E}\left([W(t) - w_0]^2\right) = t - t_0. \quad (\text{A.17})$$

Since the Weiner process exhibits Markovian evolution, the joint probability distribution becomes

$$p(\Delta w_n; \Delta w_{n-1}; \dots \Delta w_1; \Delta w_0) = \prod_{i=1}^n \left[(2\pi\Delta t)^{-1/2} \exp(-\Delta w_i^2 / 2\Delta t_i) \right] p(w_0, t_0) \quad (\text{A.18})$$

which demonstrates the crucial property of independent increments, namely each $\Delta W_i = W(t_i) - W(t_{i-1})$ remains independent for all times. In particular, we have

$$\begin{aligned} E(W(t)W(s)|W_0, t_0) &= E([W(t) - W(s)]W(s)) + E(W(s)^2) \\ &= \min(t - t_0, s - t_0) + w_0^2. \end{aligned} \quad (\text{A.19})$$

Returning to eq.(A.5), we can now write

$$\int_0^t ds \xi(s) = u(t) = W(t) \quad (\text{A.20})$$

telling us that eq.(A.1) only makes sense as an integral relation,

$$\begin{aligned} x(t) - x(0) &= \int_0^t ds a(x(s), s) + \int_0^t ds b(x(s), s) \xi(s) \\ &= \int_0^t ds a(x(s), s) + \int_0^t dW b(x(s), s). \end{aligned} \quad (\text{A.21})$$

In the second line of eq.(A.21) we have defined a new structure “ $\int dW(t)$ ” to denote an integral over a measure that contains a stochastic random variable. Even though we have arrived at the connection between $u(t)$ and $W(t)$ through the usual Riemann-Stieltjes integral, the integration over dW must have some other non-trivial interpretation.

A.2 Ito's lemma and stochastic calculus

In order to uncover the meaning behind integrating over dW , suppose that we have an arbitrary deterministic function of time, $F(t)$, and Weiner process $W(t)$. We start by defining the stochastic integral as a limit of partial sums,

$$S_n = \sum_{i=1}^n F(\tau_i) [W(t_i) - W(t_{i-1})]. \quad (\text{A.22})$$

with $t_i \leq \tau_i \leq t_{i+1}$. Based on the independence of increments, we find the curious relationship that the partial sum will depend on the particular choice of intermediate point τ_i . If we define $\tau_i = \alpha t_i + (1 - \alpha)t_{i-1}$ with $0 < \alpha < 1$ and replace $F(t)$ with the Weiner process $W(t)$, we have

$$\begin{aligned} E(S_n) &= E \left(\sum_{i=1}^n W(\tau_i) [W(t_i) - W(t_{i-1})] \right) \\ &= \sum_i^n (\tau_i - t_{i-1}) = \alpha(t - t_0), \end{aligned} \quad (\text{A.23})$$

implying that the mean value sits anywhere between 0 and $t - t_0$. By choosing $\tau_i = t_i$ we obtain the Ito stochastic integral defined in the mean-square limit,

$$\int dW(t')F(t') = \text{ms-} \lim_{n \rightarrow \infty} \sum_i^n F(t_{i-1}) [W(t_i) - W(t_{i-1})]. \quad (\text{A.24})$$

While the Ito integral is not a unique definition of a stochastic integral, the relations implied by the Ito definition naturally fit the behaviour of most physical and financial systems. We will use the Ito definition for the remainder of this paper without further qualification⁶.

As an example of the application of Ito calculus, consider the meaning of $\int_{t_0}^t dW(t')W(t')$. Using the the partial sum definition, we have,

$$\begin{aligned} S_n &= \sum_{i=1}^n W_{i-1}(W_i - W_{i-1}) \equiv \sum_{i=1}^n W_{i-1}\Delta W_i \\ &= \frac{1}{2} [W(t)^2 - W(t_0)^2] - \frac{1}{2} \sum_{i=1}^n (\Delta W_i)^2. \end{aligned} \quad (\text{A.25})$$

By repeated application of the independent increment property of ΔW_i , we can show that

$$\text{ms-} \lim_{n \rightarrow \infty} \sum_{i=1}^n (W_i - W_{i-1})^2 = t - t_0 \quad (\text{A.26})$$

yielding the curious result

$$\int_{t_0}^t dW(t')W(t') = \frac{1}{2} ([W(t)^2 - W(t_0)^2] - (t - t_0)). \quad (\text{A.27})$$

We clearly see that the Ito stochastic integral does not behave like the usual Riemann-Stieltjes integral. The presence of the term $(t - t_0)$ arises from $|W(t + \Delta t) - W(t)| \sim \sqrt{\Delta t}$, and hence terms second order in $\Delta W(t)$ do not vanish when taking the limit. The Ito stochastic integral has several other non-intuitive properties and, in order to proceed, we will need one other relation. Again, suppose that we have some deterministic function $F(t)$ and consider the relationship implied by

$$\int_{t_0}^t [dW(t')]^{2+N} F(t') \equiv \text{ms-} \lim_{n \rightarrow \infty} \sum_i^n F_{i-1} \Delta W_i^{2+N}. \quad (\text{A.28})$$

For $N = 0$ we can write

$$\begin{aligned} I &= \lim_{n \rightarrow \infty} \text{E} \left(\left[\sum_i F_{i-1} (\Delta W_i^2 - \Delta t_i) \right]^2 \right) \\ &= \lim_{n \rightarrow \infty} \text{E} \left(\sum_i F_{i-1}^2 (\Delta W_i^2 - \Delta t_i)^2 + \sum_{i>j} 2F_{i-1}F_{j-1} (\Delta W_j^2 - \Delta t_j) (\Delta W_i^2 - \Delta t_i) \right) \end{aligned} \quad (\text{A.29})$$

⁶Other types of stochastic integrals, such as the Fisk-Stratonovich Integral, are constructed using general intermediate points. In the limit, the partial sum implied by the Ito stochastic integral can be shown to follow a martingale (a probabilistic model of a fair game) with respect to a generalized probability measure. The martingale property is commonly perceived as desirable in financial modelling.

and using $E(\Delta W_i^2) = \Delta t_i$ and $E([\Delta W_i^2 - \Delta t_i]^2) = 2\Delta t_i^2$ we have

$$I = 2 \lim_{n \rightarrow \infty} \sum_i \Delta t_i^2 E((F_{i-1})^2) \quad (\text{A.30})$$

leading to

$$\text{ms-} \lim_{n \rightarrow \infty} \left(\sum_{i=1}^n F_{i-1} \Delta W_i^2 - \sum_{i=1}^n F_{i-1} \Delta t_i \right) = 0. \quad (\text{A.31})$$

Thus, in the mean-square limit we find,

$$\int_{t_0}^t [dW(t')]^2 F(t') = \int_{t_0}^t dt' F(t') \quad (\text{A.32})$$

implying that the stochastic integral over $[dW(t')]^2$ has collapsed to the usual Riemann-Stieltjes integral over dt' . We can therefore make the identification

$$dW(t)^2 \rightarrow dt. \quad (\text{A.33})$$

In a similar fashion, we can show that $dW(t)^N \rightarrow 0$ for $N > 2$ and $dW(t)dt \rightarrow 0$. We see that when manipulating differential stochastic terms, we must retain factors up to order two in calculations. For example, the total derivative of an arbitrary function, $f(W(t), t)$ yields,

$$\begin{aligned} df(W(t), t) &= \frac{\partial f}{\partial t} dt + \frac{\partial f}{\partial W} dW + \frac{1}{2} \frac{\partial^2 f}{\partial t^2} (dt)^2 + \frac{1}{2} \frac{\partial^2 f}{\partial W^2} (dW)^2 + \frac{\partial^2 f}{\partial t \partial W} (dt)(dW) \\ &= \left(\frac{\partial f}{\partial t} + \frac{1}{2} \frac{\partial^2 f}{\partial W^2} \right) dt + \frac{\partial f}{\partial W} dW. \end{aligned} \quad (\text{A.34})$$

If we now imagine a general stochastic process $dx(t) = a(x, t)dt + b(x, t)dW$, as heuristically depicted in figure A.1, we arrive at Ito's Lemma for change of variable,

$$df[x(t)] = \left(a[x(t), t]f'[x(t)] + \frac{1}{2}b^2[x(t), t]f''[x(t)] \right) dt + b[x(t), t]f'[x(t)]dW(t). \quad (\text{A.35})$$

The model construction presented in this paper requires the connection of the Fokker-Planck equation to the SDE. Using Ito's Lemma, we have for an arbitrary function, $f(x)$ with $dx(t) = a(x, t)dt + b(x, t)dW$

$$\frac{d}{dt} E(f(x(t))) = E \left(a[x(t), t] \frac{\partial f}{\partial x} + \frac{1}{2} b^2[x(t), t] \frac{\partial^2 f}{\partial x^2} \right) \quad (\text{A.36})$$

and, since $x(t)$ has a conditional probability density $p(x, t|x_0, t_0)$, we also have

$$\begin{aligned} \frac{d}{dt} E(f[x(t)]) &= \int dx f(x) \frac{\partial}{\partial t} p(x, t|x_0, t_0) \\ &= \int dx \left(a[x(t), t] \frac{\partial f}{\partial x} + \frac{1}{2} b^2[x(t), t] \frac{\partial^2 f}{\partial x^2} \right) p(x, t|x_0, t_0). \end{aligned} \quad (\text{A.37})$$

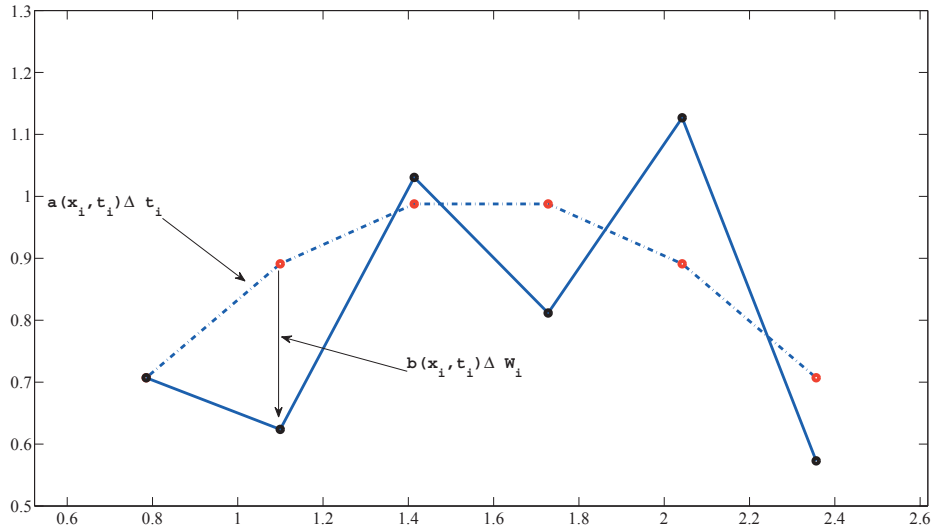


Figure A.1: Stochastic behaviour depicted using an Euler-Cauchy approximation. Each time increment contains two pieces: a deterministic drift part and a stochastic fluctuation.

Based on the arbitrariness of $f(x)$, and after integration by parts, we obtain the desired link between the Fokker-Planck equation and the SDE, namely,

$$\frac{\partial}{\partial t} p(x, t | x_0, t_0) = -\frac{\partial}{\partial x} (a[x(t), t] p(x, t | x_0, t_0)) + \frac{1}{2} \frac{\partial^2}{\partial x^2} (b^2[x(t), t] p(x, t | x_0, t_0)). \quad (\text{A.38})$$

The solution to eq.(A.38) yields the probability distribution of the system affording us an indirect method of modelling the process numerically.

List of Acronyms

| | |
|----------|---|
| ACF | Autocorrelation Function |
| ADM(Mat) | Assistant Deputy Minister (Materiel) |
| Ao | Operational Availability |
| CFM | Cost Factors Manual |
| CORA | Centre for Operational Research and Analysis |
| DAEBM | Director Aerospace Equipment Business Management |
| DGAEPM | Director General Aerospace Equipment Program Management |
| DMGOR | Directorate Materiel Group Operational Research |
| DND | Department of National Defence |
| DRDC | Defence Research and Development Canada |
| GARCH | Generalized Autoregressive Conditional Heteroscedasticity |
| O&M | Operation and Maintenance |
| SDE | Stochastic Differential Equation |
| USAF | United States Airforce |
| USN | United States Navy |

Distribution list

DRDC CORA TR 2009–001

Internal distribution

- 1 Chief Scientist DRDC CORA
- 1 Section Head (Joint and Common OR)
- 1 Section Head (Air)
- 1 DASOR
- 1 ORAD
- 1 CFAWC ORT
- 1 DRDC CORA Library
- 6 Spares (held by author)

Total internal copies: 13

External distribution

Department of National Defence

- 1 COS Mat
- 1 DCOS Mat
- 1 DGAEPM
- 1 COS DGAEPM

Total external copies: 4

Total copies: 17

This page intentionally left blank.

DOCUMENT CONTROL DATA

(Security classification of title, body of abstract and indexing annotation must be entered when document is classified)

| | | | |
|--|--|---|--|
| 1. ORIGINATOR (The name and address of the organization preparing the document. Organizations for whom the document was prepared, e.g. Centre sponsoring a contractor's report, or tasking agency, are entered in section 8.) Defence R&D Canada – CORA Dept. of National Defence, MGen G.R. Pearkes Bldg., 101 Colonel By Drive, Ottawa, Ontario, Canada K1A 0K2 | | 2. SECURITY CLASSIFICATION (Overall security classification of the document including special warning terms if applicable.) UNCLASSIFIED | |
| 3. TITLE (The complete document title as indicated on the title page. Its classification should be indicated by the appropriate abbreviation (S, C or U) in parentheses after the title.) Optimal Fleet Replacement and Forecasting Under Uncertainty | | | |
| 4. AUTHORS (Last name, followed by initials – ranks, titles, etc. not to be used.) Maybury, D.W. | | | |
| 5. DATE OF PUBLICATION (Month and year of publication of document.) March 2009 | 6a. NO. OF PAGES (Total containing information. Include Annexes, Appendices, etc.) 70 | 6b. NO. OF REFS (Total cited in document.) 27 | |
| 7. DESCRIPTIVE NOTES (The category of the document, e.g. technical report, technical note or memorandum. If appropriate, enter the type of report, e.g. interim, progress, summary, annual or final. Give the inclusive dates when a specific reporting period is covered.) Technical Report | | | |
| 8. SPONSORING ACTIVITY (The name of the department project office or laboratory sponsoring the research and development – include address.) Defence R&D Canada – CORA Dept. of National Defence, MGen G.R. Pearkes Bldg., 101 Colonel By Drive, Ottawa, Ontario, Canada K1A 0K2 | | | |
| 9a. PROJECT NO. (The applicable research and development project number under which the document was written. Please specify whether project or grant.) N/A | 9b. GRANT OR CONTRACT NO. (If appropriate, the applicable number under which the document was written.) | | |
| 10a. ORIGINATOR'S DOCUMENT NUMBER (The official document number by which the document is identified by the originating activity. This number must be unique to this document.) DRDC CORA TR 2009–001 | 10b. OTHER DOCUMENT NO(s). (Any other numbers which may be assigned this document either by the originator or by the sponsor.) | | |
| 11. DOCUMENT AVAILABILITY (Any limitations on further dissemination of the document, other than those imposed by security classification.) (X) Unlimited distribution () Defence departments and defence contractors; further distribution only as approved () Defence departments and Canadian defence contractors; further distribution only as approved () Government departments and agencies; further distribution only as approved () Defence departments; further distribution only as approved () Other (please specify): | | | |
| 12. DOCUMENT ANNOUNCEMENT (Any limitation to the bibliographic announcement of this document. This will normally correspond to the Document Availability (11). However, where further distribution (beyond the audience specified in (11)) is possible, a wider announcement audience may be selected.) | | | |

13. ABSTRACT (A brief and factual summary of the document. It may also appear elsewhere in the body of the document itself. It is highly desirable that the abstract of classified documents be unclassified. Each paragraph of the abstract shall begin with an indication of the security classification of the information in the paragraph (unless the document itself is unclassified) represented as (S), (C), (R), or (U). It is not necessary to include here abstracts in both official languages unless the text is bilingual.)

Using the CP-140A Arcturus maritime surveillance aircraft as a case study, we examine fleet replacement and overhaul decisions by applying the same stochastic techniques used to price financial derivatives. We construct a stochastic fleet replacement/overhaul model with forecasting capabilities for the CP-140A using historical operation and maintenance costs along with historical operational availability trends. Our model uses a class of utility functions based on operational availability for discounting purposes, and the model balances tradeoffs between costs, availability, and uncertainty. We find that the effects of uncertainty in both costs and availability play a non-trivial role in establishing the optimal replacement time. Through the underlying stochastic process driving the fleet costs, we develop forecast envelopes using the parameters of the model. We see this model as having potential for application to other fleets, systems, and subsystems that exhibit stochastic operation and maintenance costs.

14. KEYWORDS, DESCRIPTORS or IDENTIFIERS (Technically meaningful terms or short phrases that characterize a document and could be helpful in cataloguing the document. They should be selected so that no security classification is required. Identifiers, such as equipment model designation, trade name, military project code name, geographic location may also be included. If possible keywords should be selected from a published thesaurus. e.g. Thesaurus of Engineering and Scientific Terms (TEST) and that thesaurus identified. If it is not possible to select indexing terms which are Unclassified, the classification of each should be indicated as with the title.)

Fleet Replacement
Life-Cycle Costing
Forecasting
Stochastic Differential Equation
CP-140A Arcturus
Mean First Passage Time
Bellman's Principle



www.drdc-rddc.gc.ca